


University of Alberta

Observer-Based Fault Detection for Induction Motors

by

Guiying Yu 

A thesis submitted to the Faculty of Graduate Studies and Research
in partial fulfillment of the requirements for the degree of

Master of Science

Department of Electrical and Computer Engineering

Edmonton, Alberta
Fall 2006



Library and
Archives Canada

Bibliothèque et
Archives Canada

Published Heritage
Branch

Direction du
Patrimoine de l'édition

395 Wellington Street
Ottawa ON K1A 0N4
Canada

395, rue Wellington
Ottawa ON K1A 0N4
Canada

Your file *Votre référence*
ISBN: 978-0-494-22413-7
Our file *Notre référence*
ISBN: 978-0-494-22413-7

NOTICE:

The author has granted a non-exclusive license allowing Library and Archives Canada to reproduce, publish, archive, preserve, conserve, communicate to the public by telecommunication or on the Internet, loan, distribute and sell theses worldwide, for commercial or non-commercial purposes, in microform, paper, electronic and/or any other formats.

The author retains copyright ownership and moral rights in this thesis. Neither the thesis nor substantial extracts from it may be printed or otherwise reproduced without the author's permission.

AVIS:

L'auteur a accordé une licence non exclusive permettant à la Bibliothèque et Archives Canada de reproduire, publier, archiver, sauvegarder, conserver, transmettre au public par télécommunication ou par l'Internet, prêter, distribuer et vendre des thèses partout dans le monde, à des fins commerciales ou autres, sur support microforme, papier, électronique et/ou autres formats.

L'auteur conserve la propriété du droit d'auteur et des droits moraux qui protègent cette thèse. Ni la thèse ni des extraits substantiels de celle-ci ne doivent être imprimés ou autrement reproduits sans son autorisation.

In compliance with the Canadian Privacy Act some supporting forms may have been removed from this thesis.

Conformément à la loi canadienne sur la protection de la vie privée, quelques formulaires secondaires ont été enlevés de cette thèse.

While these forms may be included in the document page count, their removal does not represent any loss of content from the thesis.

Bien que ces formulaires aient inclus dans la pagination, il n'y aura aucun contenu manquant.


Canada

Abstract

The subject of this thesis is the development of model based fault detection (FD) techniques for induction motors.

During the past twenty years, several techniques for induction motor fault detection have been developed. Most of them are signal-based and knowledge-based methods. With the development of advanced modern control theory, it is possible to develop model-based FD techniques for induction motors since the induction motor model is understood. The purpose of this thesis is to develop model-based schemes for induction motor fault detection. Specifically, observers are employed to detect the faults. Robustness to disturbances is also considered. The motor model is tested on a laboratory experimental setup.

The motor faults considered in this thesis are shorted stator windings and broken rotor bars. Since they are hard to simulate on a physical motor because of the damage, a PC-based real-time simulator is used to simulate the motor under faulty conditions, and the designed FD schemes are then implemented on it.

Acknowledgements

This project has been a great challenge and a wonderful learning experience. I would like to express sincere appreciation to Dr. Qing Zhao and Dr. Venkata Dinavahi for their help, assistance and excellent supervision during my graduate studies. Without their help, this thesis would not have come to existence or at least the time producing it would have been much longer.

I would like to acknowledge the Department of Electrical and Computer Engineering, University of Alberta, for giving me the opportunity to pursue my graduate study. I also would like to give my thanks to the staff and many of the graduate students of the Department of Electrical and Computer Engineering for their support and help.

Special thanks to my husband Peijun for being patient and supportive during the busy years of my study.

Contents

1	Introduction	1
1.1	Overview	2
1.2	Objectives	3
1.3	Outline of the Thesis	4
2	Literature Review	7
2.1	Existing Techniques for Induction Motor Fault Detection	8
2.1.1	Signal-Based Fault Detection Techniques for Induction Motors	8
2.1.2	Knowledge-Based Fault Detection Techniques for Induction Motors	9
2.1.3	Model-Based Fault Detection	11
2.2	Observer-Based Residual Generation	13
2.2.1	Luenberger Observers	13
2.2.2	Unknown Input Observers	15
2.3	Real-Time Simulation	16
3	Induction Motor Modeling and Experimental Validation	18
3.1	Modeling of the Squirrel Cage Induction Motor	19
3.2	Induction Motor Model in Arbitrary dq Reference Frames	23
3.2.1	Motor Model in Stationary Frame	25
3.2.2	Motor Model in Synchronously Rotating Frame	25
3.2.3	Mechanical System	26
3.2.4	A State-Space Model of the Induction Motor	26
3.3	Simulation of Induction motor	28
3.4	Experimental Validation of Induction Motor Model	32
3.4.1	Experiment Setup	32
3.4.2	Experimental Results	34
3.5	Modeling of Faults	35
4	Fault Detection Observer Design for Induction Motors	40
4.1	Bilinear Observer Based Fault Detection	41
4.1.1	A Bilinear Observer	41
4.1.2	Bilinear Observer Design for Induction Motors	43
4.1.3	Stability Analysis of Bilinear Observers	46

4.1.4	Experimental Validation of the Convergency of the Bi-linear Observer	49
4.2	Unknown Input Observers	50
4.2.1	Theory of Unknown Input Observers	50
4.2.2	Design of An Unknown Input Observer for Fault Detection of Induction Motors	54
5	Implementation of Induction Motor Fault Detection	63
5.1	RT-Lab Real-time Simulation Software	64
5.2	Real-time Simulation Results	66
6	Conclusions	73
6.1	Conclusions	74
6.2	Recommendations for Further Work	75
	Bibliography	77

Chapter 1

Introduction

1.1 Overview

The induction motor (IM) has a wide range of applications in various industries to convert electrical power into mechanical power, for example, in pumps and ventilators. Indeed, in the industrialized countries, the entire electrical power available is mainly consumed by AC motors, wherein most are induction motors [1]. Safety, reliability, and performance are some of the major concerns of their applications. With the high reliability requirement, the issues of induction motor fault detection are of increasing importance.

Usually, a fault detection scheme makes use of the available knowledge (model) of the system in normal operations to generate (compute) an output signal of interest. When faults occur in the system, by comparing the true measurement of the output signal and the estimated one based on the system knowledge (model) in normal operations, discrepancies can be obtained which is also called the residual (signal). Such a residual can indicate the abnormal conditions of the system caused by faults. Fault detection can be performed by checking the “size” of the residual. In an ideal case where there are no unknown inputs or disturbances, fault detection follows a simple logic: if the residual is zero, then there are no faults present; otherwise faults occurred. This idea of fault detection is also referred to as “analytical redundancy” compared to “hardware redundancy” for detecting the faults. The major advantage of the analytical redundancy method is that no additional hardware components are required to realize a fault detection algorithm. The algorithm can be implemented via software on the same computers used for process control. In many cases, the measurements necessary to control the process are also sufficient for the fault detection algorithm so that no additional sensors have to be installed [2].

Fault detection of induction motors has concentrated on sensing failures in one of three major components, the stator, the rotor, and the bearings. Ap-

proaches to fault detection can be classified into three groups: signal-based techniques, knowledge-based techniques, and model-based techniques. This thesis will focus on model-based techniques, particularly for induction motors. Due to the development of advanced model control theory, model-based approaches to fault detection in dynamic systems have been receiving more and more attention over the last 30 years. However, compared to signal-based and knowledge-based techniques, they are relative new in the area of fault detection for induction motor and only account for 10% of the literature. This is because induction motors are highly nonlinear systems, while most model-based fault detection techniques are for linear systems.

In general, nonlinear model-based fault detection is hard or even impossible. However, by considering specific types of nonlinear models, different techniques for model-based nonlinear fault detection method can be developed. In this thesis, the induction motor is of particular interest. Despite the fact of being a highly nonlinear system, the modeling of induction motors is well understood. Furthermore, development of modern control theories make it possible to develop methods to achieve fault detection for induction motors.

Real time simulation for electric systems and drives is receiving more and more attention in recent years. It provides a low cost and yet effective way for system testing and rapid prototyping of control systems. Since induction motors with stator fault and rotor fault are hard to be simulated on a physical motor because of the damage to the motor, a real-time simulator is a good choice to simulate the induction motor in faulty conditions.

1.2 Objectives

The aim of this thesis is to develop observers to provide contributions in the field of induction motor fault detection and to apply real-time simulation to the designed schemes, more specifically, a bilinear observer and an unknown input

observer are discussed. The overall fault detection scheme is shown in Figure 1.1. Since the induction motor is modeled in a two-phase reference frame, its measurements (stator current and motor speed) are transformed into this reference frame. The observer provides the estimates of stator current and motor speed of a healthy motor. Any difference between the estimates and the real measurements will indicate a faulty condition.

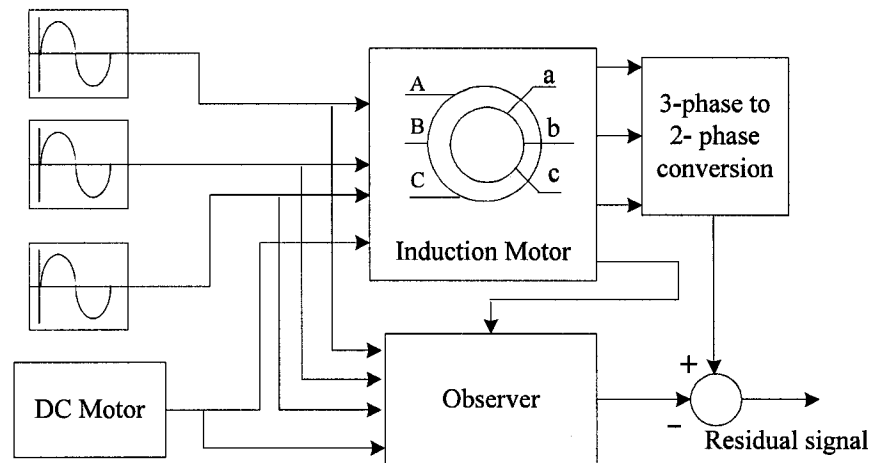


Figure 1.1: Fault detection system for an induction motor

The objectives of the thesis are as follows:

1. Develop observers that are insensitive to load disturbance and imbalance of the three phase power supply, but sensitive to considered faults.
2. Analyze the stability of the designed observers.
3. Implement the designed fault detection schemes on the RTX-LAB real-time digital simulator.

1.3 Outline of the Thesis

The thesis is organized as follows:

Chapter 2 - Literature Review

Reviews existing techniques for induction motor fault detection, and introduces some basic concepts needed later in the thesis. The design part of Chapter 4 relies heavily on theory introduced in this chapter. RTX-LAB real-time simulator, which is used in Chapter 5 is also introduced.

Chapter 3 - Induction Motor Modeling and Experimental Validation

Describes the dynamic model of a symmetrical three-phase induction motor with a squirrel cage rotor. The model is written as a fifth order, nonlinear state-space model with stator current, rotor flux and motor speed as state variables. The two phase dq reference frame is discussed. In order to perform fault detection, it is necessary to model the faults. Two types of faults, namely, stator windings fault and broken rotor bars, are considered and they are modeled as abrupt change of stator and rotor resistance, respectively. Finally, the laboratory experimental setup used to validate the mathematical model of the model is discussed. Experiments were performed on a 2hp induction motor.

Chapter 4 - Fault Detection Observer Design for Induction Motors

The induction motor fault detection is described. The purpose is to use bilinear observer and unknown input observer to generate a residual signal that is insensitive to disturbances and sensitive to fault only. First it is discussed how the bilinear observer is designed by writing the motor model in its bilinear form with the motor speed as a time-varying parameter. The stability of the linear time-varying system is analyzed based on Lyapunov method. Then the design of the unknown input observer is described. It is an extension of the linear unknown input observer, but makes the use of the complete nonlinear model of the induction motor.

Chapter 5 - Real Time Simulation

In this chapter, a fully digital real-time simulation of the observer-based fault detection schemes for an induction motor using RT-Lab software is presented. Satisfactory results are obtained with a fixed time-step of 100 μs . The chapter

starts with the RTX-LAB implementation of the observers, and a variety of simulation results under different scenarios are provided. It follows that the designed bilinear observer and unknown input observer are robust to load disturbance and power supply imbalance. This chapter ends with discussions by comparing the two observers.

Chapter 6 - Conclusions

This chapter contains conclusions and recommendations for further work.

Chapter 2

Literature Review

The chapter reviews existing techniques for induction motor fault detection. The basic concepts of model based fault detection and the RTX-LAB real-time simulator needed in this thesis later are also included.

2.1 Existing Techniques for Induction Motor Fault Detection

Induction motors are widely used equipment of many industrial processes. Safety, reliability, and performance are some of the major concerns of its applications. With the high reliability requirement, issues of induction motor fault detection and diagnosis are of increasing importance. For these reasons, during the past twenty years, there have been continually increasing interests and investigation on induction motor fault detection and diagnosis. Fault detection and diagnosis schemes for induction motors are intended to provide advanced warnings of the incipient faults, so that corrective action can be taken to prevent economical losses or danger for the personnel working in the industrial environment.

In general, fault detection scheme of induction motors is concentrated on sensing failures in one of the three major components, the stator, the rotor, and the bearings. Approaches to detection of those faults can be classified into three groups: signal-based techniques, knowledge-based techniques, and model-based techniques.

2.1.1 Signal-Based Fault Detection Techniques for Induction Motors

The most commonly used signal-based fault detection technique is motor current signature analysis, known as MCSA. This method analyzes motor current to detect faults in a three-phase induction motor while it is still operating. The

first progress toward the development of an online stator winding fault monitor using MCSA was proposed by Williamson and Mirzoian [5], and the majority of the methods developed since then to detect insulation failures are based on this technique. MCSA is based on the fact that faults will have effects on the spectrum of the motor current and thus can be detected by analyzing the spectral components. Based on this technique, the motor current spectrum has been monitored to detect mechanical failure related to stator winding problems (insulation degradation, breakdown leading to short-circuits, etc.), eccentricity or broken rotor bars [8]-[10].

However, owing to the following difficulties, practical application of MCSA is much more complicated and many problems have not been solved [11].

- There are other components that may exist in the stator current spectrum, for example, harmonics because of supply voltage distortion or load variations, and harmonics caused by background noise.
- The current spectrum is very sensitive to the accuracy of line frequency measurement.
- Induction motors are driven by power electronics systems. Normally these power electronic controllers have robust stabilization ability, thus a motor fault may not show up because of the controller. In other words, the inner fault is covered by the perfect performance of the controller [11]. This makes signal-based approaches more difficult to apply.

2.1.2 Knowledge-Based Fault Detection Techniques for Induction Motors

Artificial Neural Network (ANN) is another method used for induction motor fault detection. It was first proposed by Chow et al. [13]. They have primarily considered incipient faults for single-phase motors. [14] proposed the use of ANN for identifying different types of external faults on three-phase induction

motors. A variety of schemes based on ANN have been developed since then. In [15], the ANN techniques including feed-forward back propagation networks (FFBPN) and self organizing maps (SOM), are investigated. Common induction motor faults such as bearing faults, stator winding faults, unbalanced rotor and broken rotor bars are considered. The ANNs were trained and tested using dynamic measurements of stator currents and mechanical vibration signals. The effects of different network structures and the training set sizes on the performance of the ANNs are discussed. In [16], vibration analysis has been employed to study the health conditions of a brand new 1.5 hp squirrel cage induction motor. Two types of faults were selected for study: the bearing fault, which was simulated by a mechanical modification on the front bearing house; and the imbalance in supply, which was simulated by adjusting the supply voltages. In recent years, pattern recognition technique based on ANN is playing a significant role to identify the incipient faults of induction motors. Such a scheme has been proposed to detect the incipient faults of induction motors in [17]. The design, implementation and dynamic updating of this type of system has been illustrated with an example.

Neural networks are very good modeling tools for highly non-linear systems. Due to this modeling abilities, neural network is an ideal method for generating residuals. The main drawback is due to the difficulties to perform neural network training [2]. For example, ANN should be trained by a number of samples before it can be used for diagnosis. The samples for training have important effect on the performance of the ANN and therefore should be carefully chosen. A solution to this problem is made by Chow [18], who combined the Fuzzy and ANN technology into the diagnosis system. The trained system can not only provide accurate fault detection, but also provide the heuristics with the use of fuzzy rules and fuzzy member functions. It has better performance than ANN. However, the system is still sensitive to load and other interference. Another drawback of artificial neural networks is their lack of transparency in human understandable terms [2]. These weaknesses have limited their applications.

2.1.3 Model-Based Fault Detection

Model-based approach to fault detection in dynamic systems has been receiving more and more attention over the last 30 years. The basic idea of model-based fault detection is to use an accurate model of the system to mimic the real process behavior. If a fault occurs, the residual signal, which indicates the difference between the real system and the model behaviors, can be used to identify the faults. Figure 2.1 gives a schematic description of the model-based fault detection and diagnosis scheme. The key of this approach lies in the use of the process model. The process model (e.g., an observer) represents the fault-free process. Driven by the same process input, the process model delivers an estimation of the measured process variables. Comparing the estimated outputs with the measured outputs yields the so-called residual signals, and faults are thus detected by setting fixed or variable thresholds on residual signals.

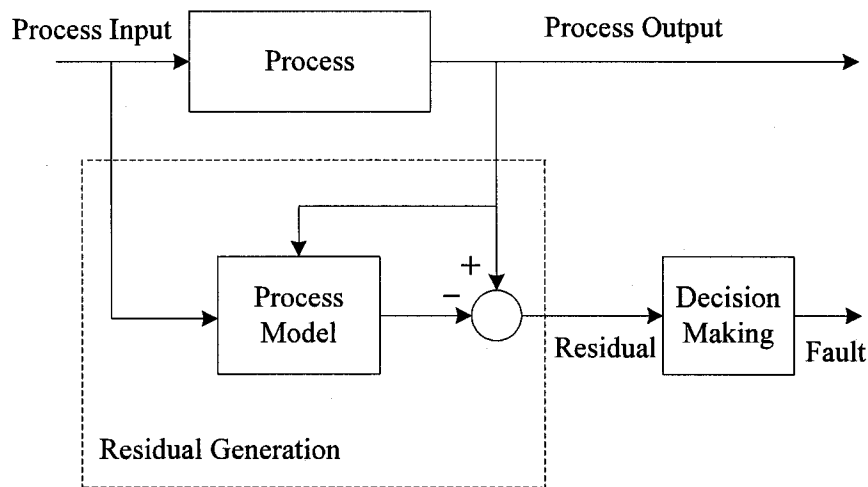


Figure 2.1: Structure of model-based fault detection scheme

The major advantage of model-based fault detection is that no additional hardware components are required in order to realize a fault detection algorithm. A model-based fault detection algorithm can be implemented via software on the same computers used for process control. In many cases, the

measurements necessary to control the process are also sufficient for the fault detection algorithm so that no additional sensors have to be installed [2]. Under these circumstances, only additional storage capacity and possibly greater computer power is needed for the implementation of a model-based fault detection algorithm. This saves money, space and gives more reliability. However, a perfectly accurate mathematical model of a physical system is never available. There is always a mismatch between the actual process and its mathematical model even under no fault conditions. This causes difficulties in its applications because this may cause false alarms and missed alarms [2]. To overcome this problem, a number of methods have been proposed in the literature, for example, the Unknown Input Observer(UIO) [22].

Model-based fault detection in general consists of two steps: residual generation and decision making.

a) Residual generation Residual generation is the key part of this approach. The purpose is to generate a fault indicating signal, called residual, using available inputs and outputs from the process. This residual should indicate that a fault has occurred. It should normally be zero or close to zero under no fault condition, whilst distinguishably different from zero when a fault occurs. This means that the residual is characteristically independent of process inputs and outputs in ideal conditions.

b) Decision making The generated residuals are examined for the likelihood of faults and a decision rule is then applied to determine if any faults have occurred. A decision rule can be a simple threshold test on the instantaneous values or moving averages of the residuals. For instance, in an ideal case where there are no model uncertainties and no disturbances, a decision rule could be a simple logic: if the residual is zero, then no faults; otherwise, faults occurred.

The generation of residuals is the main part of model-based fault detection. The design of fault indication signals is normally achieved through a comparison between measured signals with their estimates, where the estimates are

generated using the mathematical model of the process.

2.2 Observer-Based Residual Generation

A variety of methods are available in literature for residual generation and most commonly used methods are parameter estimation, parity equations, and observer-based approaches. They are well-known techniques and a comprehensive survey of these methods can be found in [2]. In this thesis, the scope is limited to observer-based residual generation.

The basic idea behind the observer-based residual generation is to estimate the outputs of the system from the measurements by using Luenberger observers, unknown input observers (UIO), Beard fault detection filter (BFDF), combined UIO and BFDF, eigen-structure assignment method, etc. [32] [53]. The output estimation error is therefore used as residual. This thesis will focus on Luenberger observer based and unknown input observer based methods for nonlinear systems. Some basic results on these two types of observers for linear systems are reviewed first.

2.2.1 Luenberger Observers

A device that estimates or observes state variables of a system is called a state observer. A state observer utilizes measurements of the system inputs and outputs and a model of the system based on differential or difference equations. In the deterministic case, when no random noise is present, the Luenberger observer is used for time-invariant systems with known parameters. Consider a n -dimensional state equation

$$\begin{aligned}\dot{x}(t) &= Ax(t) + Bu(t) \\ y(t) &= Cx(t) + Du(t)\end{aligned}\tag{2.1}$$

where $A \in R^{n \times n}$, $B \in R^{n \times p}$, $C \in R^{m \times n}$, and $D \in R^{m \times p}$ are given matrices. The input $u(t) \in R^{p \times 1}$ and the output $y(t) \in R^{m \times 1}$ are available. The state vector $x(t) \in R^{n \times 1}$, however, is not available. The Luenberger observer estimates state $x(t)$ from $u(t)$ and $y(t)$ with the knowledge of A, B, and C, as shown in equation (2.2).

$$\begin{aligned}\dot{\hat{x}}(t) &= A\hat{x}(t) + Bu(t) + L[y(t) - \hat{y}(t)] \\ \hat{y}(t) &= C\hat{x}(t) + Du(t)\end{aligned}\tag{2.2}$$

where $\hat{x}(t)$ is the estimate of the state $x(t)$, $L \in R^{n \times m}$ is a constant gain matrix. The Luenberger observer contains a correcting term $L[y(t) - \hat{y}(t)]$, which reflects the difference between the actual measurement and the estimation of the current output. If the difference is zero, no correction is needed. If the difference is nonzero, with the gain L properly designed, the difference will drive the estimated state to the actual state. Inclusion of this correction term ensures stability and convergence of the observer even when the system being observed is unstable.

Define the error between the actual state and the estimated state as

$$e(t) = x(t) - \hat{x}(t)$$

It follows that

$$\dot{e}(t) = (A - LC)e(t)\tag{2.3}$$

Equation (2.3) governs the estimation error. If all eigenvalues of $A - LC$ can be assigned arbitrarily, then we can control the rate for $e(t)$ to approach zero or, equivalently, for the estimated state to approach actual state.

Luenberger observers are typically used for linear time-invariant systems and the system matrices A, B, and C are assumed exactly known. However, a perfect model of the system is never available. When there exist model uncertainties, the estimation error may not approach to zero and the Luenberger

observer may even become unstable. In this case, an unknown input observer (UIO) is a good choice for state estimation and fault detection.

2.2.2 Unknown Input Observers

The most important task in model-based fault detection is the generation of residuals which are independent of disturbances [2]. Unknown input observer is the most commonly used approach to achieve this goal. The principle of UIO is to make the output estimation error (residual) decoupled from the unknown inputs or disturbances. Uncertainties in system modeling can be considered as unknown inputs. Although the unknown inputs vector is unknown, its distribution matrix is usually assumed known.

This approach was originally proposed by Watanabe and Himmelblau [19], who considered the sensor fault detection problem for systems with modeling uncertainties. Later, the approach was generalized by Patton [20] and Frank [21] in order to perform fault detection for both sensors and actuators. Very important contributions to this subject made by Patton et al. can be found in [22], where the structure of a full order UIO for fault detection purpose was obtained and the necessary and sufficient existence conditions as well as the design procedure were given. The details of UIO theory will be described in Section 4.2 of this thesis.

Model-based approach to fault detection in dynamic systems has been receiving more and more attention over the last 30 years. However, compared to signal-based and knowledge-based techniques, it is relatively new in the applications of induction motor fault detection. It only accounts for 10% of the literature. In [23], a diagnostic procedure for induction motors working in closed loop was developed. It uses a nonlinear tracking controller made of an observer and a feedback-linearizing module to generate residual signals used for fault diagnosis. In [24], a model-based fault detection and diagnosis system

was compared to the more traditional signal-based motor fault estimator. It was shown that the model-based one has better performance in terms of mitigating the adverse effects caused by false alarms. [3] showed that an induction motor could be represented by a bilinear model and a bilinear observer was designed to detect current sensor faults.

2.3 Real-Time Simulation

With the increasing complexity of power electronic systems and their wide use in industries, and with the increasing pressure for reduced time-to-market and costs, the need for extensive simulation is inevitable. Real-time simulation of electric systems and drives plays an important role in rapid prototyping and testing of new circuit topologies and control strategies [25].

Digital real-time simulation has been used for years and many commercial products have been developed. However, the real-time simulation of electrical systems presents a challenge for several reasons. The main reason is that electrical systems have higher bandwidth than mechanical systems and therefore command smaller simulation time steps [26]. RT-Lab from Opal-RT Technologies provides a good solution to this problem. It can currently work at a sampling time below $10\mu s$ [27]. It is now widely used by high-tech industries, including electric systems and drives [25] - [28], automotive [29] - [30], and aeronautics industries (aircraft flight control, satellite control), as the main tool for rapid prototyping of complex engineering systems in a cost-effective and secure manner, while reducing the time-to-market.

RT-Lab is a distributed digital real-time platform. A typical configuration of RT-Lab consists of command stations, target nodes, the communication links (FireWire and Ethernet), and I/O boards, as shown in figure 2.2. The command station servers as the user interface for accessing the targets, and is used for editing and modifying models. The target nodes are real-time processing

and communication computers interconnected by an Ethernet adapter. These computers can also include a real-time communication interface like FireWire, as well as I/O boards for accessing external equipment.

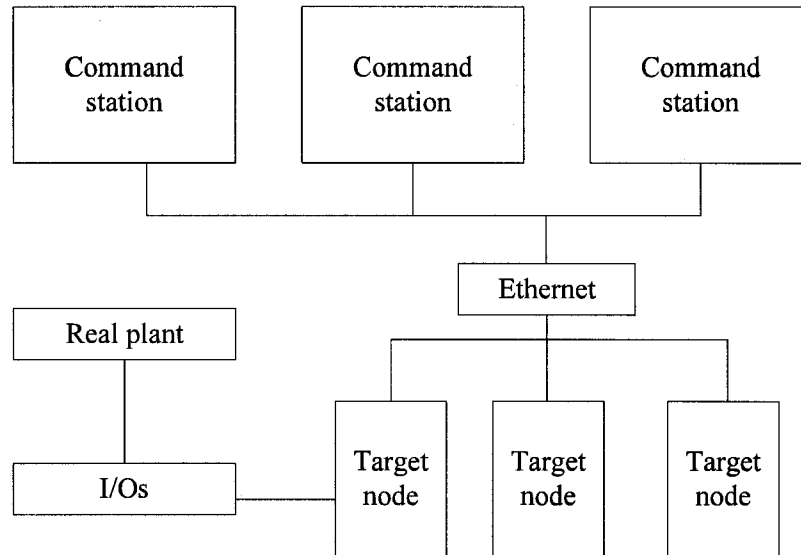


Figure 2.2: Configuration of RT-Lab

RT-Lab uses the popular Matlab/Simulink as a front-end for editing and viewing graphic models in block-diagram format. The block diagrams made with Matlab/Simulink first have to be separated into subsystems and inserted appropriate communication blocks. Each subsystem is then automatically coded in C program and compiled for execution by the target node. Once the compilation is done, RT-lab automatically distributes its calculations among the target processors [31].

In this thesis, the real-time simulation of the designed induction motor fault detection scheme is performed and is successfully implemented in RT-Lab software package. Satisfactory results are obtained with a fixed time-step of $100\mu\text{s}$.

Chapter 3

Induction Motor Modeling and Experimental Validation

In this chapter, modeling of induction motors and induction motor faults is presented, and the experimental validation of the model is performed. First, in Section 3.1, the voltage equations and flux equations of an induction motor with squirrel cage rotor and three star connected stator windings are derived in three-phase frame (*abc* frame), using magnetic coupled circuit theory [33]. A number of assumptions are made in order to obtain a simple model. Because those equations are in motor natural frame (three-phase frame), they contain time-varying parameters, making it not a practical model. To eliminate the time-varying terms, in Section 3.2, the model in three phase frame is transformed into a two-phase *dq* reference frame. The induction motor *dq* model is derived both in stationary reference frame and synchronously rotating reference frame. In order to allow an observer-based fault detection scheme, a state-space model of the induction motor is also derived in this section. Section 3.3 includes the simulation results of the motor model in stationary reference frame and synchronously rotating reference frame. It shows that the *dq* quantities are constants in steady-state in the synchronously rotating reference frame and it will be our choice for the rest of the thesis.

An experiment is performed on a laboratory system with a 2 HP induction motor, and the results are given in Section 3.4. Section 3.5 describes the modeling of the faults. Two types of faults, broken rotor bars and shorted-circuit in stator windings, are considered. They are modeled as abrupt changes in rotor resistance and stator resistance, respectively.

3.1 Modeling of the Squirrel Cage Induction Motor

This section describes the dynamic model of a symmetrical three-phase induction motor with a squirrel cage rotor. The induction motor mainly consists of two parts, the stator and the rotor. Figure 3.1 shows a cross-section view of a three phase, squirrel caged induction motor [35].

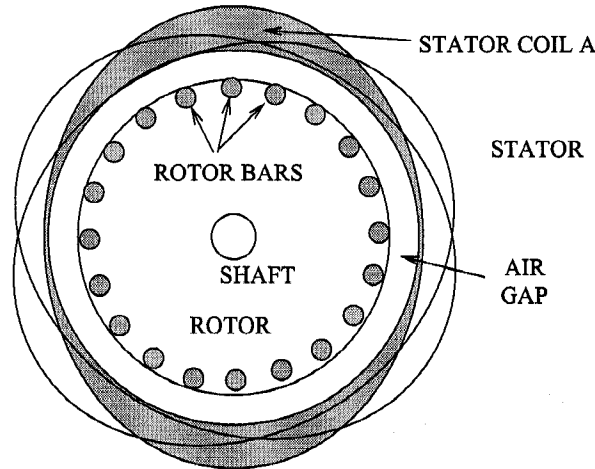


Figure 3.1: Cross-section View of Induction Motor [35]

The rotor is rotating inside the stator separated by an air gap, and the rotor is built from parallel conductors short-circuited by a ring at each end, as shown in Figure 3.2 [35]. Such a rotor can be represented by a three-phase rotor winding with short-circuits at the end. The windings of the three stator coils (A, B and C) are distributed sinusoidally displaced by 120 degrees. The stator shown is of the one-pole pair type, meaning that the coils will produce one magnetic north and one magnetic south pole. Often a motor will be constructed with several pole pairs by connecting coils in parallel and displacing the coils by $120/n_p$ degrees, where n_p is the number of pole pairs. This works as a gearing giving a larger torque and a slower mechanical rotational speed.

The stator windings are supplied with sinusoidal voltages to create a rotating magnetic field. When the rotor and the magnetic field of the stator rotate at different speeds, currents will be induced in the rotor windings. These currents result in a magneto-motive force perpendicular to the current and to the magnetic field resulting in a torque on the rotor.

A common approach to modeling induction machine is to use the magnetic coupled circuit theory [34]. The machine is described as a set of multiple cou-

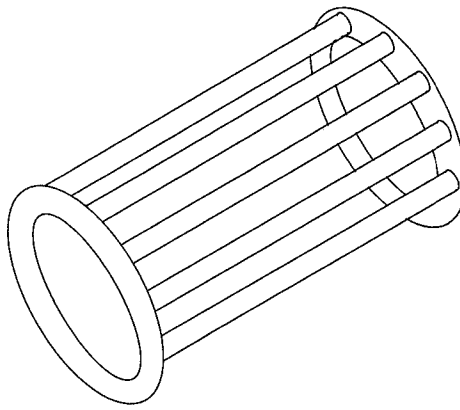


Figure 3.2: Squirrel Cage Rotor [35]

pled circuits defined by self- and mutual- inductances. The result is a set of differential equations, some of which are non-linear. This is not very practical due to the complexity.

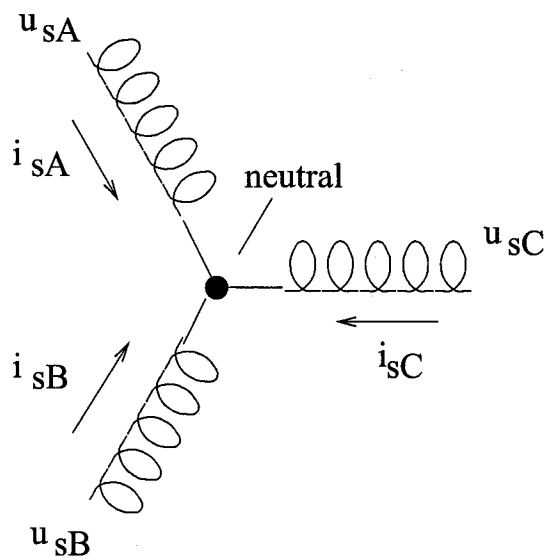


Figure 3.3: Star connected stator windings [35]

To obtain a simplified model, a number of assumptions are made in practice. Classical assumptions include that [35]:

- The motor is symmetrical.

- The rotor is concentric and the air gap has a constant width.
- The stator windings are star connected (see Figure 3.3) and the neutral is isolated.
- The ends of the rotor bars are short circuited.
- The flux density is radial in the air gap.
- The coil resistances and inductances are constant.

One simplification resulting from these assumptions is that the rotor can be treated as three phase short-circuited windings distributed the same way as the stator coil. With the above assumptions, the voltage equations and the flux equations of the magnetically coupled stator and rotor windings can be written in matrix form as [34]:

$$\begin{aligned}
v_{sabc} &= \bar{R}_s i_{sabc} + p \lambda_{sabc} \\
v_{rabc} &= \bar{R}_r i_{rabc} + p \lambda_{rabc} = 0 \\
\lambda_{sabc} &= \bar{L}_s i_{sabc} + \bar{M}_{sr}(\theta_r) i_{rabc} \\
\lambda_{rabc} &= \bar{L}_r i_{rabc} + \bar{M}_{rs}(\theta_r) i_{sabc}
\end{aligned} \tag{3.1}$$

where $v_{abc}=[v_a \ v_b \ v_c]^T$ represents voltage, $i_{abc}=[i_a \ i_b \ i_c]^T$ the current, $\lambda_{abc}=[\lambda_a \ \lambda_b \ \lambda_c]^T$ the flux, $\bar{R}=\text{diag}\{R \ R \ R\}$ the resistance. The subscript “s” represents stator quantities, while “r” rotor quantities. \bar{L}_s and \bar{L}_r are matrices of stator-to-stator and rotor-to-rotor winding inductances and are given in [34]. To differentiate from dq frame later, the subscript “abc” is used for the abc frame. $\bar{M}_{sr}(\theta_r)$ and $\bar{M}_{rs}^T(\theta_r)$ are the matrices representing the mutual inductances between the stator and the rotor. They are dependent on the rotor angle, that is

$$\begin{aligned}
\bar{M}_{sr}(\theta_r) &= \bar{M}_{rs}^T(\theta_r) \\
&= L_{sr} \begin{bmatrix} \cos(n_p \theta_r) & \cos(n_p \theta_r + \frac{2}{3}\pi) & \cos(n_p \theta_r - \frac{2}{3}\pi) \\ \cos(n_p \theta_r - \frac{2}{3}\pi) & \cos(n_p \theta_r) & \cos(n_p \theta_r + \frac{2}{3}\pi) \\ \cos(n_p \theta_r + \frac{2}{3}\pi) & \cos(n_p \theta_r - \frac{2}{3}\pi) & \cos(n_p \theta_r) \end{bmatrix}
\end{aligned}$$

where n_p is the number of pole pairs, L_{sr} the peak value of stator to rotor mutual inductance, θ_r the angle between the axes of the stator and the rotor. Denote ω_r the rotor electrical rotating speed in radian, then θ_r can be expressed as

$$\theta_r(t) = \int_0^t \omega_r(t) dt + \theta_r(0)$$

Note that for the idealized machine, those equations are coupled through the mutual inductances between the windings. In particular, the stator-to-rotor coupling terms are a function of rotor position; thus, when the rotor rotates, these coupling terms vary with time.

To eliminate the time-varying inductances, in power electronic, induction machine model is transformed into an arbitrary dq reference frame, in which the differential equations with time-varying inductances become differential equations with constant inductances.

3.2 Induction Motor Model in Arbitrary dq Reference Frames

The idealized three phase induction machine model has time-varying terms, and the dq transformation is used to facilitate the computation. abc frame to dq frame transformation is shown in Figure 3.4. Depending on the rotating speed of the dq axes, two reference frames are commonly used in the analysis of induction machines. They are stationary reference frame, which is fixed to the stator, and synchronously rotating reference frame, which is rotating with the synchronous frequency. Each has an advantage for some purpose. Stationary reference frame is a natural choice for the supply network, thus in this frame, the dq variables of the motor are the same as those of the supply. It is convenient when the supply network is large or complex [34]. In the synchronously rotating reference frame, the dq variables become constant in steady-state. It is a convenient choice for fault detection purpose.

A formal mathematical derivation of machine model in dq reference frames can be found in [34]. The following transformation converts the motor quantities from abc frame (motor natural frame) to an arbitrary dq reference frame, which is rotating at an angular speed of ω_e .

$$T_{dq}(\theta) = \frac{2}{3} \begin{bmatrix} \cos(\theta) & \cos(\theta - \frac{2}{3}\pi) & \cos(\theta + \frac{2}{3}\pi) \\ \sin(\theta) & \sin(\theta - \frac{2}{3}\pi) & \sin(\theta + \frac{2}{3}\pi) \end{bmatrix} \quad (3.2)$$

where θ is the angle between the q -axis of the reference frame and the a -axis of the stationary stator winding. It can be expressed as follows:

$$\theta(t) = \int_0^t \omega_e(t) dt + \theta(0)$$

Applying transformation (3.2) to (3.1), the motor model in stationary reference frame and synchronously rotating reference frame can be derived by setting $\omega_e = 0$, and $\omega_e = \omega_s$, respectively, where ω_s is the synchronous angular speed.

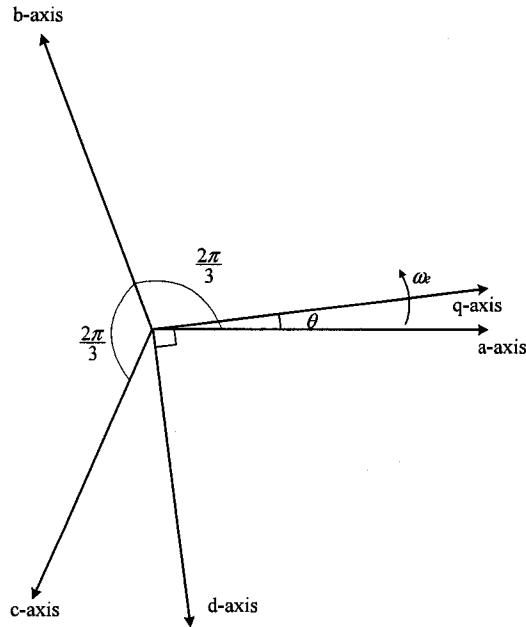


Figure 3.4: abc/dq frame transformation

3.2.1 Motor Model in Stationary Frame

Since the stationary frame is fixed to stator, its rotating speed is zero. By applying transformation (3.2) to (3.1) and setting $\omega_e = 0$, the voltage equations and flux equations can be obtained as follows:

- Voltage equations in stationary reference frame

$$v_{qs} = p\lambda_{qs} + R_s i_{qs} \quad (3.3)$$

$$v_{ds} = p\lambda_{ds} + R_s i_{ds} \quad (3.4)$$

$$v_{qr} = p\lambda_{qr} - \omega_r \lambda_{dr} + R_r i_{qr} = 0 \quad (3.5)$$

$$v_{dr} = p\lambda_{dr} + \omega_r \lambda_{qr} + R_r i_{dr} = 0 \quad (3.6)$$

- Flux equations in stationary reference frame

$$\lambda_{qs} = L_s i_{qs} + L_m i_{qr} \quad (3.7)$$

$$\lambda_{ds} = L_s i_{ds} + L_m i_{dr} \quad (3.8)$$

$$\lambda_{qr} = L_r i_{qr} + L_m i_{qs} \quad (3.9)$$

$$\lambda_{dr} = L_r i_{dr} + L_m i_{ds} \quad (3.10)$$

where subscript “dq” represent the dq component of corresponding quantities and L_m the magnetizing inductance.

3.2.2 Motor Model in Synchronously Rotating Frame

By applying transformation (3.2) to (3.1) and setting $\omega_e = \omega_s$, the voltage equations and flux equations in synchronously rotating frame can be obtained as follows:

- Voltage equations in synchronously rotating frame

$$v_{qs} = p\lambda_{qs} + R_s i_{qs} + \omega_s \lambda_{ds} \quad (3.11)$$

$$v_{ds} = p\lambda_{ds} + R_s i_{ds} - \omega_s \lambda_{qs} \quad (3.12)$$

$$v_{qr} = p\lambda_{qr} + (\omega_s - \omega_r) \lambda_{dr} + R_r i_{qr} = 0 \quad (3.13)$$

$$v_{dr} = p\lambda_{dr} - (\omega_s - \omega_r) \lambda_{qr} + R_r i_{dr} = 0 \quad (3.14)$$

- Flux equations in synchronously rotating frame

$$\lambda_{qs} = L_s i_{qs} + L_m i_{qr} \quad (3.15)$$

$$\lambda_{ds} = L_s i_{ds} + L_m i_{dr} \quad (3.16)$$

$$\lambda_{qr} = L_r i_{qr} + L_m i_{qs} \quad (3.17)$$

$$\lambda_{dr} = L_r i_{dr} + L_m i_{ds} \quad (3.18)$$

3.2.3 Mechanical System

The mechanical rotational speed ω_m is affected by the electro-magnetic torque T_e and the load torque T_L .

$$J \frac{d\omega_m}{dt} = T_e + T_L \quad (3.19)$$

where

$$\begin{aligned} T_e &= \frac{3}{2} n_p (\lambda_{qr} i_{dr} - \lambda_{dr} i_{qr}) \\ &= \frac{3}{2} n_p (\lambda_{ds} i_{qs} - \lambda_{qs} i_{ds}) \\ &= \frac{3}{2} n_p L_m (i_{dr} i_{qs} - i_{qr} i_{ds}) \end{aligned} \quad (3.20)$$

where n_p is the number of pole pairs. J is the collective moment of inertia of the rotor and the load, assuming the shaft to be rigid. T_L contains the actual load along with the speed-dependent viscous and coulomb friction. The electrical rotational speed ω_r is defined as

$$\omega_r = \dot{\theta}_r = n_p \omega_m \quad (3.21)$$

Equations (3.3) to (3.21) form the model used in motor simulation given in section 3.3 and the state space model used in observer design.

3.2.4 A State-Space Model of the Induction Motor

In this section, a state-space model of induction motor is given, which is to be used for the observer design.

The state space model of the induction motor depends on the selection of the reference frame. Since the dq variables in synchronously rotating frame are constants in steady state, we shall use this frame to derive the state-space model.

Equation (3.11) to (3.20) represent the dynamics of the induction motor in synchronously rotating frame. Re-write them in state space form as:

$$\begin{aligned}\dot{x}(t) &= f(x(t)) + Bu(t) \\ y(t) &= Cx(t)\end{aligned}\quad (3.22)$$

where

$$\begin{aligned}x &= [x_1 \ x_2 \ x_3 \ x_4 \ x_5]^T \\ &= [i_{qs} \ i_{ds} \ \lambda_{qs} \ \lambda_{ds} \ \omega]^T \\ f(x(t)) &= \begin{bmatrix} -\gamma x_1(t) + \alpha \beta x_3(t) - n_p \beta x_5(t) x_4(t) - \omega_s x_2(t) \\ -\gamma x_2(t) + \alpha \beta x_4(t) + n_p \beta x_5(t) x_3(t) + \omega_s x_1(t) \\ \alpha L_m x_1(t) - \alpha x_3(t) + n_p x_5(t) x_4(t) - \omega_s x_4(t) \\ \alpha L_m x_2(t) - \alpha x_4(t) - n_p x_5(t) x_3(t) + \omega_s x_3(t) \\ \frac{3}{2} n_p \frac{L_m}{J L_r} (x_4(t) x_1(t) - x_3(t) x_2(t)) + \frac{1}{J} T_L \end{bmatrix}\end{aligned}$$

$$B = \begin{bmatrix} \frac{1}{\sigma L_s} & 0 \\ 0 & \frac{1}{\sigma L_s} \\ 0 & 0 \\ 0 & 0 \\ 0 & 0 \end{bmatrix}$$

$$C = \begin{bmatrix} 1 & 0 & 0 & 0 & 0 \\ 0 & 1 & 0 & 0 & 0 \\ 0 & 0 & 0 & 0 & 1 \end{bmatrix}$$

$$\sigma = 1 - \frac{L_m^2}{L_s L_r}, \quad \alpha = \frac{R_r}{L_r},$$

$$\beta = \frac{L_m}{\sigma L_s L_r}, \quad \gamma = \frac{L_m^2 R_r}{\sigma L_s L_r^2} + \frac{R_s}{\sigma L_s}$$

The rest of the symbols used are listed in table 3.1.

This is a fifth-order, highly nonlinear model because of the coupling between the mechanical part (motor mechanical speed) and the electrical part (rotor fluxes). This state-space model shall be used in observer design in chapter 4.

3.3 Simulation of Induction motor

In this section, the simulation study of the induction motor model developed in section 3.2 is carried out. To do so, equation (3.3) - (3.21) have to be rearranged to be suitable for Simulink implementation. Note that the operator p has been replaced by operator $1/s$ since Simulink deals with integrator better than with differentiator.

- **Simulation of the model in stationary reference frame**

Stator and rotor fluxes can be expressed as follows:

$$\lambda_{qs} = \frac{1}{s}(v_{qs} - R_s i_{qs}) \quad (3.23)$$

$$\lambda_{ds} = \frac{1}{s}(v_{ds} - R_s i_{ds}) \quad (3.24)$$

$$\lambda_{qr} = \frac{1}{s}(\omega_r \lambda_{dr} - R_r i_{qr}) \quad (3.25)$$

$$\lambda_{dr} = \frac{1}{s}(-\omega_r \lambda_{qr} - R_r i_{dr}) \quad (3.26)$$

Stator and rotor currents can be expressed as follows:

$$i_{qs} = \frac{L_r}{L_x} \lambda_{qs} - \frac{L_m}{L_x} \lambda_{qr} \quad (3.27)$$

$$i_{ds} = \frac{L_r}{L_x} \lambda_{ds} - \frac{L_m}{L_x} \lambda_{dr} \quad (3.28)$$

$$i_{qr} = \frac{L_s}{L_x} \lambda_{qr} - \frac{L_m}{L_x} \lambda_{qs} \quad (3.29)$$

$$i_{dr} = \frac{L_s}{L_x} \lambda_{dr} - \frac{L_m}{L_x} \lambda_{ds} \quad (3.30)$$

where $L_x = L_s L_r - L_m^2$.

- **Simulation of the model in synchronously rotating reference frame**

Stator and rotor fluxes can be expressed as follows:

$$\lambda_{qs} = \frac{1}{s}(v_{qs} - R_s i_{qs} - \omega_s \lambda_{ds}) \quad (3.31)$$

$$\lambda_{ds} = \frac{1}{s}(v_{ds} - R_s i_{ds} + \omega_s \lambda_{qs}) \quad (3.32)$$

$$\lambda_{qr} = \frac{1}{s}(\omega_r \lambda_{dr} - R_r i_{qr} - \omega_s \lambda_{dr}) \quad (3.33)$$

$$\lambda_{dr} = \frac{1}{s}(-\omega_r \lambda_{qr} - R_r i_{dr} + \omega_s \lambda_{qr}) \quad (3.34)$$

Stator and rotor currents can be expressed as follows:

$$i_{qs} = \frac{L_r}{L_x} \lambda_{qs} - \frac{L_m}{L_x} \lambda_{qr} \quad (3.35)$$

$$i_{ds} = \frac{L_r}{L_x} \lambda_{ds} - \frac{L_m}{L_x} \lambda_{dr} \quad (3.36)$$

$$i_{qr} = \frac{L_s}{L_x} \lambda_{qr} - \frac{L_m}{L_x} \lambda_{qs} \quad (3.37)$$

$$i_{dr} = \frac{L_s}{L_x} \lambda_{dr} - \frac{L_m}{L_x} \lambda_{ds} \quad (3.38)$$

- **Motor mechanical rotating speed**

From equation (3.19) to (3.21), the mechanical speed of the motor can be obtained as

$$J \frac{d\omega_m}{dt} = \frac{3}{2} n_p (\lambda_{ds} i_{qs} - \lambda_{qs} i_{ds}) + T_L \quad (3.39)$$

Note that the equation of the mechanical part is same in both reference frames.

- **Simulation Results**

Figure 3.5 shows stator phase A current responses, motor speed, and the torque, respectively, obtained from equation (3.23) to (3.39) without load. It must be said that both reference frames (stationary and synchronous) as well as the state space model give the same simulation results since they are different representations of the same motor. The validity of the motor model is thus achieved. The model will be further validated in section 3.4 in an experiment.

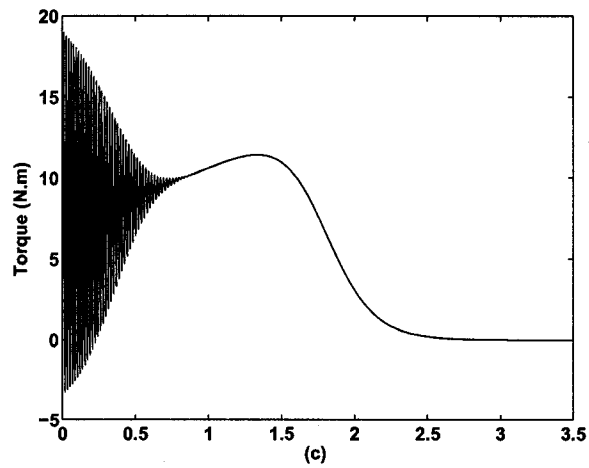
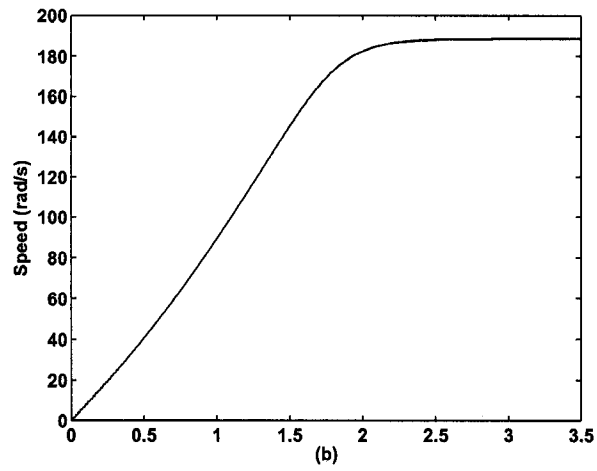
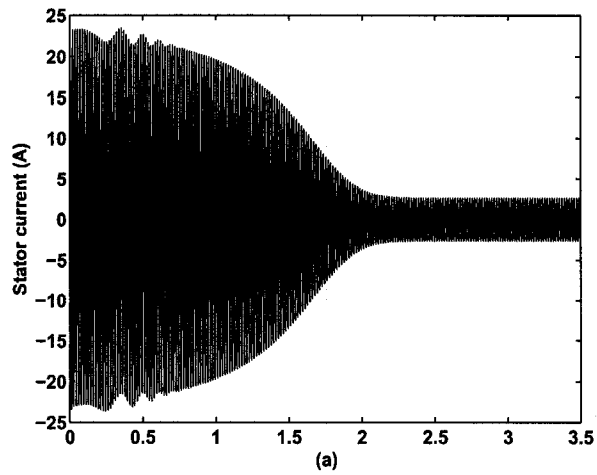


Figure 3.5: Simulation outputs of the induction motor without load (a) Stator current (b) Speed response (c) Torque response

All simulations are done in Matlab/Simulink. Motor characteristics are listed in Table 3.1.

Figure 3.6 shows the dq components of the stator phase A current in synchronous reference frame. It can be seen that the dq components of the motor quantities in synchronous frame become constants in steady state, which makes it easier to analyze the fault effects later. Therefore, we shall use the model in the synchronous reference frame for the observer design and analysis later.

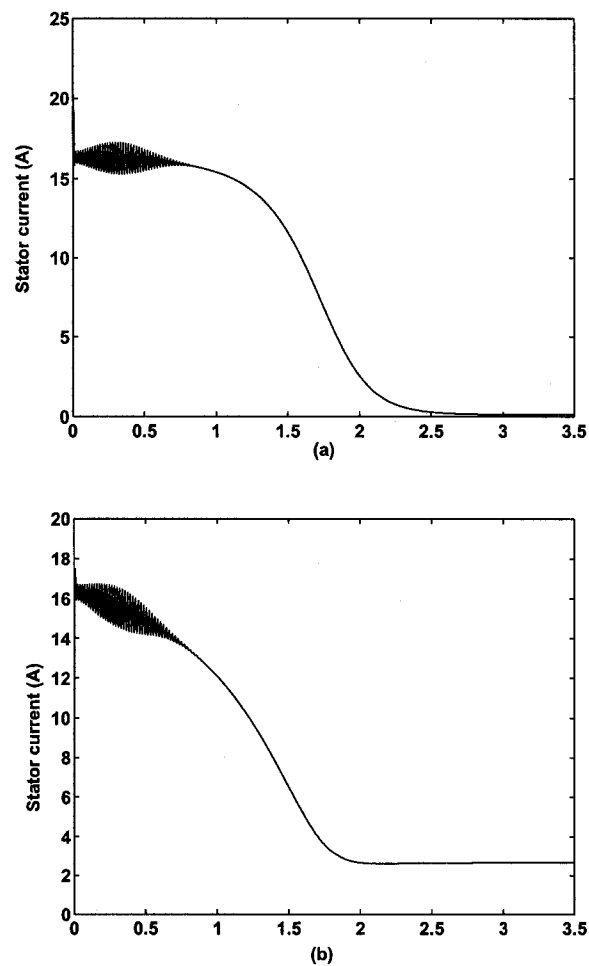


Figure 3.6: Stator current in synchronous frame (a) q component (b) d component

3.4 Experimental Validation of Induction Motor Model

In this section, an experiment is performed on a laboratory induction motor under normal operation to validate the mathematical model of the motor given in section 3.2. This can be done by comparing the actual outputs from the experiment with the simulated outputs from the mathematical model.

3.4.1 Experiment Setup

The experiment is set up as in Figure 3.7 and Figure 3.8. A PC is connected to the motor to receive and analyze the measurements, eg. stator current and motor speed. The inverter is used to provide the three-phase stator voltage. An encoder is connected to the shaft to measure the speed. The DC motor allows the simulation of load torque.

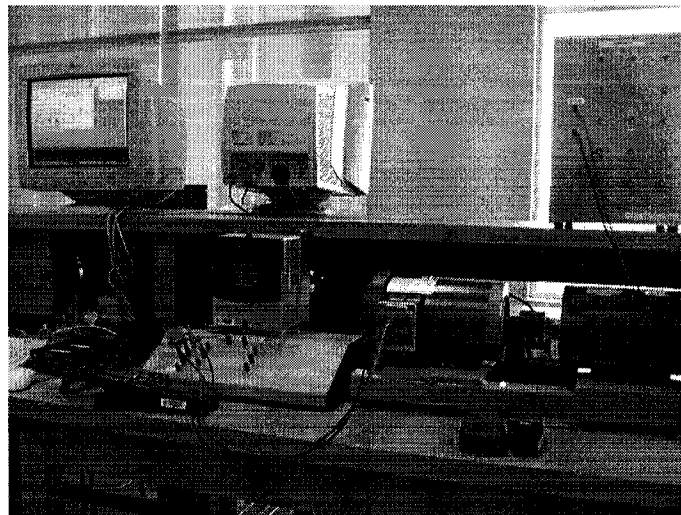


Figure 3.7: Experiment Setup

The induction motor has two pole pairs ($n_p = 2$), a squirrel-cage rotor, and three star connected stator windings. Its nominal power is 2HP. The mea-

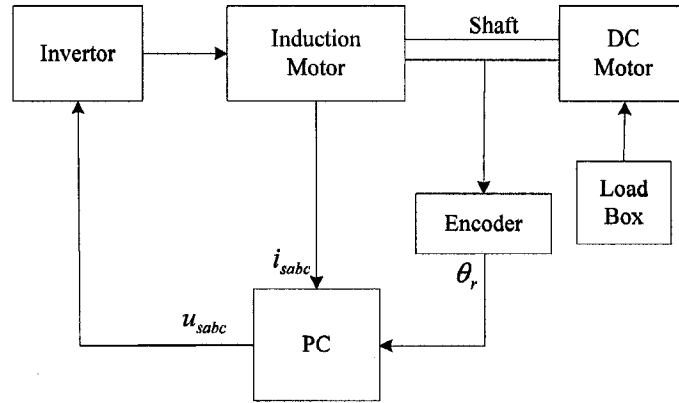


Figure 3.8: Experimental Setup

surement are stator current and motor angular speed. The parameters of the induction motor were identified as

$$R_s = 3.35\Omega, \quad R_r = 2.4\Omega, \quad L_s = 7.6e - 3H,$$

$$L_r = 8.6e - 3H, \quad L_m = 1.048e - 3H$$

All parameters are listed in Table 3.1.

Table 3.1: Induction motor parameters

Description	Param.	Values
Stator resistance	R_s	3.35 ohms
Rotor resistance	R_r	2.4 ohms
Stator inductance	L_s	7.6e-3H
Rotor inductance	L_r	8.6e-3H
Mutual inductance	L_m	1.048e-3H
Moment of inertia	J	0.01Kg.m ²
Number of pole pairs	n_p	2
Line to line Input voltage	V	208V
Stator voltage frequency	f	60Hz
Rating	S	2 HP

3.4.2 Experimental Results

The inputs of the squirrel cage induction motor are the three-phase voltages, their fundamental frequency, and the load torque. The outputs are the three-phase currents and the motor mechanical speed. However, the dq model requires all three-phase variables be transformed to the two-phase synchronously rotating frame. Consequently, the three-phase stator currents from the experiment have to be transformed to synchronous dq frame for comparison, as shown in Figure 3.9.

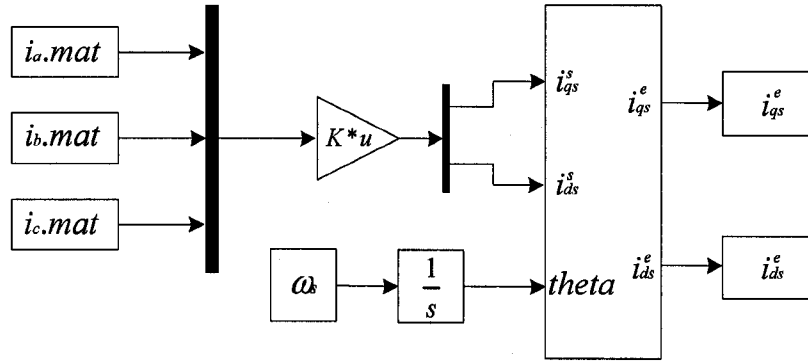


Figure 3.9: Transforming three phase stator current into synchronous dq frame

Three-phase currents are first converted to two-phase stationary frame using (3.40) and then from the stationary frame to the synchronously rotating frame using (3.41) as follows:

$$\begin{bmatrix} i_{qs}^s \\ i_{ds}^s \end{bmatrix} = \begin{bmatrix} \frac{2}{3} & -\frac{1}{3} & -\frac{1}{3} \\ 0 & -\frac{1}{\sqrt{3}} & \frac{1}{\sqrt{3}} \end{bmatrix} \begin{bmatrix} i_{as} \\ i_{bs} \\ i_{cs} \end{bmatrix} \quad (3.40)$$

$$\begin{bmatrix} i_{qs}^e \\ i_{ds}^e \end{bmatrix} = \begin{bmatrix} \cos(\theta_e) & -\sin(\theta_e) \\ \sin(\theta_e) & \cos(\theta_e) \end{bmatrix} \begin{bmatrix} i_{qs}^s \\ i_{ds}^s \end{bmatrix} \quad (3.41)$$

where the superscript “s” refers to stationary frame and superscript “e” refers to the synchronously rotating frame. The angle, θ_e is the angle between the axis of the two frames and is calculated directly by integrating the frequency

of the input three-phase voltage, ω_s .

$$\theta_e = \int_0^t \omega_s dt + \theta_e(0)$$

Figure 3.10 and Figure 3.11 show the comparison results between the experiment and the mathematical model. There is a relative big difference between the experiment and the mathematical model during the startup. This is because: 1) The rotor initial angular position is unknown in the experiment. 2) The motor model is under some assumptions. The model may not be able to capture all dynamic behaviors during startup. 3) The rotor parameters (resistance and inductance) are heavily depending on its working condition. For example, the rotor resistance will vary with the temperature. On the other hand, the outputs (stator currents) from the mathematical model are close enough to those of the experiment, despite of unknown initial rotor position and inaccurate motor parameters. Thus the mathematical model is validated. This model will be used for observer design.

3.5 Modeling of Faults

During the operation of induction motors, a number of faults of electrical and mechanical parts may occur. The four main kinds of faults in induction machines are:

1. Winding faults: short-circuits of stator windings, short-circuits of rotor windings, broken rotor bars, broken rings of the rotor.
2. Faults of the magnetic circuit: air-gap asymmetry.
3. Faults of motor mechanical system: mainly bearing failures.
4. Instrumentation faults: the encoder, voltage sensors and current sensor faults.

All these faults are connected with some particular phenomena: electrical,

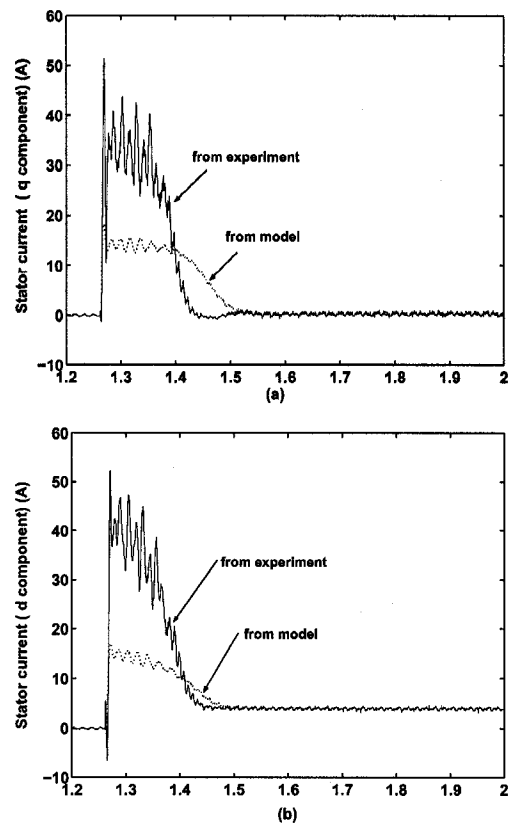


Figure 3.10: Comparison of stator phase A current (a) q component (b) d component

or magnetic.

Among the above faults, stator/rotor winding faults are the main contributor to motor failures. According to a survey [36], winding faults and bearing failures account for 46% and 40% of all motor faults, respectively, while other failures take 14%. Therefore, fault detection schemes are usually designed for the three main induction machine components: the stator, the rotor and the bearings. In this thesis, two major types of faults are considered: the broken rotor bars and shorted-circuit in stator windings.

It has been mentioned that signal-based fault detection techniques are focused on analyzing the specific components of the motor currents to detect faults. They do not need models of systems or faults. However, for model-based

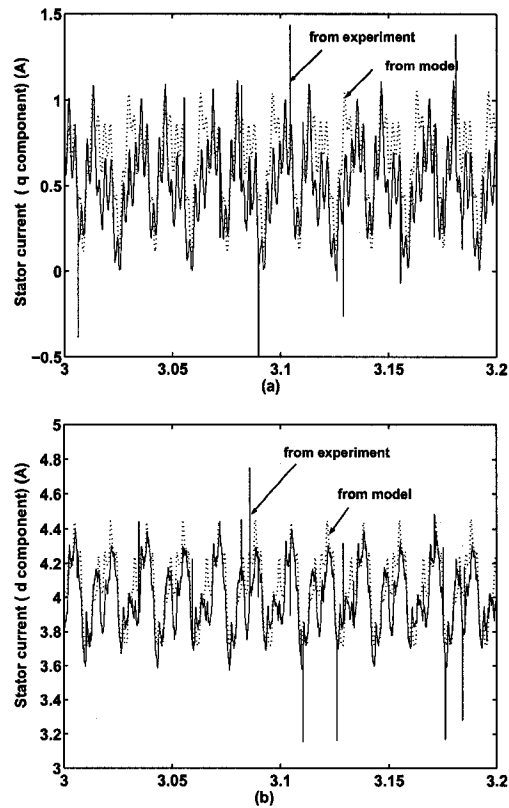


Figure 3.11: Detailed comparison of stator phase A current (a) q component (b) d component

techniques, it is necessary to model the faults. Broken rotor bars and stator winding faults have direct influences on motor parameters, and researchers have modeled them differently for specific purposes. In [23], faults are modeled as abrupt changes in stator resistance and rotor resistance, ignoring the changes in leakage inductance and mutual inductance. However, it failed to provide details of calculating those changes. In [37], broken rotor bar was modeled, but the stator winding faults were not considered. In this section, we will model the two types of faults as changes in resistances only as in [23], and give the details on how to compute the resistance changes.

- **Modeling of broken rotor bars**

Assume the motor has a total number of N rotor bars, and a number of n bars are broken per phase. In general, in this case, the self inductance and mutual inductance between the stator and the rotor will not change,

but the rotor resistance will increase.

Denoting R_{ra} , R_{rb} , and R_{rc} phase A, phase B, and phase C resistance of rotor, R_r the rotor resistance, R_{bar} the resistance of each rotor bar, R'_r the rotor resistance when there are broken bars, ΔR_r the change of rotor resistance. Usually we have

$$R_r = R_{ra} = R_{rb} = R_{rc}$$

Since rotors are in parallel connection within one phase,

$$R_r = \frac{R_{bar}}{\frac{N}{3}} = \frac{3R_{bar}}{N}$$

$$R'_r = \frac{R_{bar}}{\frac{N}{3} - n} = \frac{3R_{bar}}{N - 3n}$$

$$\Delta R_r = R'_r - R_r = \frac{3R_{bar}}{N} - \frac{3R_{bar}}{N - 3n} = \frac{3R_r}{N - 3n}n \quad (3.42)$$

- **Modeling of stator winding fault - shorted turns**

Assume the stator has a number of N turns and N_i turns are shorted. In this case, the stator resistance, self inductance, and even the mutual inductance between rotor and stator will all change. However, for simplicity, we only consider changes in resistances.

Denoting R_{sa} , R_{sb} , and R_{sc} phase A, phase B, and phase C resistance of stator, R_s the stator resistance, R'_s the stator resistance when there are shorted turns, ΔR_s the change of stator resistance. Usually we have

$$R_s = R_{sa} = R_{sb} = R_{sc}$$

$$R'_s = \frac{N - N_i}{N} R_s$$

$$\Delta R_s = R_s - R'_s = \frac{N_i}{N} R_s \quad (3.43)$$

We have modeled rotor and stator faults occurred at time t_0 as abrupt changes of the corresponding parameters in the motor model, as shown in equation (3.44).

$$\begin{aligned}R_r(t) &= R_r + \Delta R_r \cdot I(t - t_0) \\R_s(t) &= R_s + \Delta R_s \cdot I(t - t_0)\end{aligned}\tag{3.44}$$

where $I(\cdot)$ is a step function.

Chapter 4

Fault Detection Observer Design for Induction Motors

Observer-based methods for fault detection and isolation (FDI) have been widely used for systems for whose precise mathematical models can be found ([38], [39], [40] and [41]). Many of these methods, however, are based on linear observers. Because most practical systems show certain nonlinearities, these methods generally only work well within small operating range. Nonlinear observer based FDI methods have been studied in [42], [43], but most methods are only effective for specific classes of nonlinear systems. Also, the stability of the observer is difficult to guarantee [39]. In this theses, two observers, namely, a bilinear observer and an unknown input observer have been developed for the induction motor system.

4.1 Bilinear Observer Based Fault Detection

This section describes the design of a bilinear observer for induction motors. Its stability is proved.

4.1.1 A Bilinear Observer

Bilinear models form a more usable class of nonlinear system models. They are used to represent a wide variety of processes and systems including nuclear reactor systems, hydraulic drive systems, gas-burning furnace [44] and induction machines. Although the control of bilinear systems is well developed [45], [46], FDI for bilinear systems is seldom studied. In [47], Hara and Furuta considered the state estimation of bilinear systems, and presented existence conditions and design procedures for a minimal-order state observer for such systems. The same problem has been considered in [48], where the Lyapunov method was used to design a stable state observer. The norm of the estimation error in this method decays to zero exponentially irrespective of the input, although the error itself depends on the input. [49] considered bilinear systems with unknown inputs, and presented the design of robust state observers of

full order and minimal order. Recently, a general approach to FDI for bilinear systems, the so-called bilinear fault detection observer (BFDO) method, was proposed in [50] and a reduced order bilinear fault detection observer, which is an extension of the linear unknown input observer, was successfully applied to a furnace system for residual generation [51].

Consider the following bilinear system:

$$\dot{x}(t) = [A_0 + \sum_{i \in I} p_i(t) A_i] x(t) + [B_0 + \sum_{j \in J} q_j(t) B_j] u(t) \quad (4.1)$$

$$y(t) = Cx(t) \quad (4.2)$$

where $x(t) \in R^n$, $u(t) \in R^p$, and $y(t) \in R^m$ are system state, input and output, respectively; $I = \{1, \dots, i_{max}\}$, $J = \{1, \dots, j_{max}\}$; $A_0, A_i \in R^{n \times n}$; $B_0, B_j \in R^{n \times p}$; $p_i(t)$ and $q_j(t)$ are inputs or time-varying components lying within certain bounds, that is,

$$p_i^- \leq p_i(t) \leq p_i^+, i \in I \quad (4.3)$$

$$q_j^- \leq q_j(t) \leq q_j^+, j \in J \quad (4.4)$$

For system (4.1) and (4.2), an observer which reconstructs the state $x(t)$ using measurement $y(t)$ and input $u(t)$ is given as follows:

$$\begin{aligned} \dot{\hat{x}}(t) &= [A_0 + \sum_{i \in I} p_j(t) A_i] \hat{x}(t) + [B_0 + \sum_{j \in J} q_j(t) B_j] u(t) \\ &\quad - [L_0 + \sum_{i \in I} p_i(t) L_i] (y(t) - \hat{y}(t)) \end{aligned} \quad (4.5)$$

$$\hat{y}(t) = C\hat{x}(t) \quad (4.6)$$

where $\hat{x}(t) \in R^n$ is the state estimate; $L_0, L_i \in R^{n \times m}$ are observer gain matrices to be designed.

Define the estimation error as:

$$e(t) = x(t) - \hat{x}(t) \quad (4.7)$$

Then, the estimation error $e(t)$ satisfies the following equation:

$$\begin{aligned}
\dot{e}(t) &= \dot{x}(t) - \dot{\hat{x}}(t) \\
&= [A_0 + \sum_{i \in I} p_i(t)A_i]e(t) + [L_0 + \sum_{i \in I} p_i(t)L_i](y(t) - \hat{y}(t)) \\
&= (A_0 + \sum_{i \in I} p_i(t)A_i + L_0C + \sum_{i \in I} p_i(t)L_iC)e(t) \\
&= [(A_0 + L_0C) + \sum_{i \in I} p_i(t)(A_i + L_iC)]e(t) \tag{4.8}
\end{aligned}$$

It follows from (4.8) that if L_0 and L_i are constructed so that

$$(A_0 + L_0C) + \sum_{i \in I} p_i(t)(A_i + L_iC)$$

is stable for all $p_i(t)$ satisfying (4.3), then $\hat{x}(t)$ will converge to $x(t)$.

4.1.2 Bilinear Observer Design for Induction Motors

In order to design a bilinear observer, we re-write the induction motor model in a bilinear form of 4.1 and 4.2.

The induction motor represented by (3.22) is highly nonlinear because of the coupling between the electrical part and the mechanical part. How to decouple them is an interesting research topic. Since the motor mechanical speed is measurable in our case, it can be treated as an input parameter. Thus the induction motor in (3.22) becomes a fourth order linear time-varying system:

$$\dot{x}_1 = -\gamma x_1 + \alpha\beta x_3 - n_p\beta\omega x_4 - \omega_s x_2 \tag{4.9}$$

$$\dot{x}_2 = -\gamma x_2 + \alpha\beta x_4 + n_p\beta\omega x_3 + \omega_s x_1 \tag{4.10}$$

$$\dot{x}_3 = \alpha L_m x_1 - \alpha x_3 + n_p\omega x_4 - \omega_s x_4 \tag{4.11}$$

$$\dot{x}_4 = \alpha L_m x_2 - \alpha x_4 - n_p\omega x_3 + \omega_s x_3 \tag{4.12}$$

Rewrite above equations in matrix form as:

$$\dot{x}(t) = A(\omega(t)) + Bu(t) \tag{4.13}$$

$$y(t) = Cx(t) \tag{4.14}$$

where

$$x = [x_1 \ x_2 \ x_3 \ x_4]^T$$

$$A(\omega) = \begin{bmatrix} -\gamma & -\omega_s & \alpha\beta & -n_p\beta\omega \\ \omega_s & -\gamma & n_p\beta\omega & \alpha\beta \\ \alpha L_m & 0 & -\alpha & n_p\omega - \omega_s \\ 0 & \alpha L_m & -n_p\omega + \omega_s & -\alpha \end{bmatrix}$$

$$B = \begin{bmatrix} \frac{1}{\sigma L_s} & 0 \\ 0 & \frac{1}{\sigma L_s} \\ 0 & 0 \\ 0 & 0 \end{bmatrix}$$

$$C = \begin{bmatrix} 1 & 0 & 0 & 0 & 0 \\ 0 & 1 & 0 & 0 & 0 \end{bmatrix}$$

Further inspection of matrix A shows that it has a bilinear structure, and this can be seen clearly as follows:

$$\begin{aligned} \dot{x} &= (A + N\omega)x + Bu \\ y &= Cx \end{aligned} \tag{4.15}$$

where

$$A = \begin{bmatrix} -\gamma & -\omega_s & \alpha\beta & 0 \\ \omega_s & -\gamma & 0 & \alpha\beta \\ \alpha L_m & 0 & -\alpha & -\omega_s \\ 0 & \alpha L_m & \omega_s & -\alpha \end{bmatrix} = \begin{bmatrix} A_{11} & A_{12} \\ A_{21} & A_{22} \end{bmatrix}$$

$$N = \begin{bmatrix} 0 & 0 & 0 & -n_p\beta \\ 0 & 0 & n_p\beta & 0 \\ 0 & 0 & 0 & n_p \\ 0 & 0 & -n_p & 0 \end{bmatrix} = \begin{bmatrix} N_{11} & N_{12} \\ N_{21} & N_{22} \end{bmatrix}$$

where A_{ij} and N_{ij} , $i = 1, 2$, $j = 1, 2$ are 2×2 submatrices by partitioning A and N. The motor mechanical speed ω is an input parameter.

A full order Luenberger-type observer is designed as:

$$\begin{aligned}\dot{\hat{x}} &= (A + N\omega)\hat{x} - L(\omega)(y - \hat{y}) + Bu \\ \hat{y} &= C\hat{x}\end{aligned}\tag{4.16}$$

where $L(\omega)$ is the observer gain. Generally, it is a function of the bilinear input parameter ω . We write the observer gain in the following form :

$$L(\omega) = L_1 + L_2\omega$$

The error dynamics of the designed bilinear observer becomes:

$$\begin{aligned}\dot{e} &= \dot{x} - \dot{\hat{x}} \\ &= (A + N\omega)e + (L_1 + L_2\omega)(y - \hat{y}) \\ &= (A + N\omega + L_1C + L_2C\omega)e \\ &= [(A + L_1C) + (N + L_2C)\omega]e \\ &= A_e(\omega)e\end{aligned}\tag{4.17}$$

The design objective is to design L_1 and L_2 such that the above autonomous state equation is stable.

L_1 and L_2 are designed such that

$$L_1C = \begin{bmatrix} -A_{11} + \Delta & 0 \\ -A_{21} & 0 \end{bmatrix} \quad \text{and} \quad L_2C = \begin{bmatrix} -N_{11} & 0 \\ -N_{21} & 0 \end{bmatrix}$$

Hence,

$$A + L_1C = \begin{bmatrix} \Delta & A_{12} \\ 0 & A_{22} \end{bmatrix}, \quad N + L_2C = \begin{bmatrix} 0 & N_{12} \\ 0 & N_{22} \end{bmatrix}$$

Finally,

$$\begin{aligned}
A_e(\omega) &= A + L_1C + (N + L_2C)\omega \\
&= \begin{bmatrix} \Delta & A_{12} + N_{12}\omega \\ 0 & A_{22} + N_{22}\omega \end{bmatrix} \\
&= \begin{bmatrix} -\lambda_1 & 0 & \alpha\beta & -n_p\beta\omega \\ 0 & -\lambda_2 & n_p\beta\omega & \alpha\beta \\ 0 & 0 & -\alpha & n_p\omega - \omega_s \\ 0 & 0 & \omega_s - n_p\omega & -\alpha \end{bmatrix} \quad (4.18)
\end{aligned}$$

where $\Delta = \text{diag}\{-\lambda_1, -\lambda_2\}$, λ_1 and λ_2 are two positive constants.

It can be shown that the eigenvalues of the observer error dynamics are $-\lambda_1$, $-\lambda_2$, and a pair of complex conjugate, $-\alpha \pm j(\omega_s - n_p\omega)$. The first two eigenvalues can be assigned arbitrarily, but the last two are not assignable. They are determined by motor parameters, and are located in the left-half s-plane since α is positive. So all four eigenvalues can be placed in the left-half of s-plane. Generally speaking, for a time-varying system, negative eigenvalues can not guarantee the stability. However, for induction motors, stability can be achieved because the time-varying parameter, motor speed, changes much slower than the states, the error of stator current and the error of rotor flux. The next section gives a proof of stability of the designed bilinear observer.

4.1.3 Stability Analysis of Bilinear Observers

Consider a positive Lyapunov function for system (4.17):

$$V(e, \omega) = e^T F(\omega) e > 0 \quad (4.19)$$

where

$$F(\omega) = \text{diag}\{f_i(\omega)\}, \quad f_i(\omega) > 0, \quad i = 1, 2, 3, 4$$

then

$$\dot{V} = e^T [A_e^T(\omega)F(\omega) + F(\omega)A_e^T(\omega) + \dot{F}(\omega)]e$$

For induction motors, the motor speed ω is changing much slow and it can be treated as a slowly time-varying parameter. Assume that

$$\dot{F}(\omega) = \text{diag}\{\dot{f}_i(\omega)\} = 0, \quad i = 1, 2, 3, 4$$

then

$$\begin{aligned} \dot{V} &= e^T [A_e^T(\omega)F(\omega) + F(\omega)A_e^T(\omega)]e \\ &= e^T P(\omega)e \end{aligned}$$

To make $\dot{V} < 0$, we need $P(\omega)$ to be negative definite for all motor speed.

Lemma 4.1 Let M be a symmetric matrix. Partition M as $M = \begin{bmatrix} A & B^T \\ B & C \end{bmatrix}$, where $A \in R^{n \times n}$ is invertible, $A > (<) 0$, $B \in R^{(m-n) \times n}$, $C \in R^{(m-n) \times (m-n)}$. $S = C - BA^{-1}B^T$ is the Schur complement of C . Then $M > (<) 0$ if and only if $S > (<) 0$.

Proof:

Let x be any vector with right dimension. For any x , choose $y = -A^{-1}B^T x$.

We have

$$\begin{aligned} x^T S x &= x^T (C - BA^{-1}B^T)x \\ &= (y + A^{-1}B^T x)^T A (y + A^{-1}B^T x) + x^T (C - BA^{-1}B^T)x \\ &= y^T A y + y^T B^T x + x^T B y + x^T C x \\ &= \begin{bmatrix} y^T & x^T \end{bmatrix} \begin{bmatrix} A & B^T \\ B & C \end{bmatrix} \begin{bmatrix} y \\ x \end{bmatrix} \\ &= z^T M z \end{aligned}$$

then

$$S > 0 \iff M > 0$$

$$S < 0 \iff M < 0$$

Hence the proof.

For induction motors,

$$\begin{aligned}
P(\omega) &= A_e^T(\omega)F(\omega) + F(\omega)A_e(\omega) \\
&= \begin{bmatrix} -\lambda_1 & 0 & 0 & 0 \\ 0 & -\lambda_2 & 0 & 0 \\ \alpha\beta & n_p\beta\omega & -\alpha & \omega_s - n_p\omega \\ -n_p\beta\omega & \alpha\beta & n_p\omega - \omega_s & -\alpha \end{bmatrix} \begin{bmatrix} f_1(\omega) & 0 & 0 & 0 \\ 0 & f_2(\omega) & 0 & 0 \\ 0 & 0 & f_3(\omega) & 0 \\ 0 & 0 & 0 & f_4(\omega) \end{bmatrix} \\
&\quad + \begin{bmatrix} f_1(\omega) & 0 & 0 & 0 \\ 0 & f_2(\omega) & 0 & 0 \\ 0 & 0 & f_3(\omega) & 0 \\ 0 & 0 & 0 & f_4(\omega) \end{bmatrix} \begin{bmatrix} -\lambda_1 & 0 & \alpha\beta & -n_p\beta\omega \\ 0 & -\lambda_2 & n_p\beta\omega & \alpha\beta \\ 0 & 0 & -\alpha & n_p\omega - \omega_s \\ 0 & 0 & \omega_s - n_p\omega & -\alpha \end{bmatrix} \\
&= \begin{bmatrix} -2\lambda_1 f_1 & 0 & \alpha\beta f_1 & -n_p\beta\omega f_1 \\ 0 & -2\lambda_2 f_2 & n_p\beta\omega f_2 & \alpha\beta f_2 \\ \alpha\beta f_1 & n_p\beta\omega f_2 & -2\alpha f_3 & (\omega_s - n_p\omega)(f_4 - f_3) \\ -n_p\beta\omega f_1 & \alpha\beta f_2 & (\omega_s - n_p\omega)(f_4 - f_3) & -2\alpha f_4 \end{bmatrix} \\
&= \begin{bmatrix} A & B^T \\ B & C \end{bmatrix}
\end{aligned}$$

where

$$\begin{aligned}
A &= \begin{bmatrix} -2\lambda_1 f_1(\omega) & 0 \\ 0 & -2\lambda_2 f_2(\omega) \end{bmatrix} \\
B &= \begin{bmatrix} \alpha\beta f_1(\omega) & n_p\beta\omega f_2(\omega) \\ -n_p\beta\omega f_1(\omega) & \alpha\beta f_2(\omega) \end{bmatrix} \\
C &= \begin{bmatrix} -2\alpha f_3(\omega) & (\omega_s - n_p\omega)(f_4(\omega) - f_3(\omega)) \\ (\omega_s - n_p\omega)(f_4(\omega) - f_3(\omega)) & -2\alpha f_4(\omega) \end{bmatrix}
\end{aligned}$$

The Schur complement of C is:

$$S = \begin{bmatrix} -2\alpha f_3 + \frac{\alpha^2 \beta^2 f_1}{2\lambda_1} + \frac{n_p^2 \beta^2 \omega^2 f_2}{2\lambda_2} & (\omega_s - n_p\omega)(f_4 - f_3) - \frac{\alpha n_p \beta^2 \omega f_1}{2\lambda_1} + \frac{\alpha n_p \beta^2 \omega f_2}{2\lambda_2} \\ (\omega_s - n_p\omega)(f_4 - f_3) - \frac{\alpha n_p \beta^2 \omega f_1}{2\lambda_1} + \frac{\alpha n_p \beta^2 \omega f_2}{2\lambda_2} & -2\alpha f_4 + \frac{n_p^2 \beta^2 \omega^2 f_1}{2\lambda_1} + \frac{\alpha^2 \beta^2 f_2}{2\lambda_2} \end{bmatrix}$$

Let

$$f_1(\omega) = f_2(\omega), f_3(\omega) = f_4(\omega), \lambda_1 = \lambda_2 = \lambda$$

then

$$S(\omega) = \begin{bmatrix} \frac{\alpha^2\beta^2 + n_p^2\beta^2\omega^2}{2\lambda} f_1(\omega) - 2\alpha f_3(\omega) & 0 \\ 0 & \frac{\alpha^2\beta^2 + n_p^2\beta^2\omega^2}{2\lambda} f_1(\omega) - 2\alpha f_3(\omega) \end{bmatrix}$$

To make $S(\omega)$ negative definite, we need:

$$\frac{\alpha^2\beta^2 + n_p^2\beta^2\omega^2}{2\lambda} f_1(\omega) - 2\alpha f_3(\omega) < 0$$

i.e.

$$\begin{aligned} f_1(\omega) &< \frac{4\alpha\lambda}{\alpha^2\beta^2 + n_p^2\beta^2\omega^2} f_3(\omega) \\ &< \frac{4\lambda}{\alpha\beta^2} f_3(\omega) \end{aligned} \tag{4.20}$$

So given $f_3(\omega)$, we can always find $f_1(\omega)$ according to (4.20), such that $S(\omega)$ is negative definite. According to *Lemma 4.1*, $P(\omega)$ is negative definite. Thus stability of the bilinear observer is guaranteed. This is to say that the observer error will converge to zero in fault-free cases. On the other hand, when faults occurred, the error will be nonzero, indicating faulty conditions.

4.1.4 Experimental Validation of the Convergency of the Bilinear Observer

In order to validate the convergence of the bilinear observer, we apply the stator voltages from the experiment to the observer. The observer outputs, dq components of stator current are then compared to the experimental measurements, which have been converted into dq frame. The comparison results are shown in Fig. 4.1. It follows that the differences are very small in steady state. Thus the convergence of the designed observer is validated.

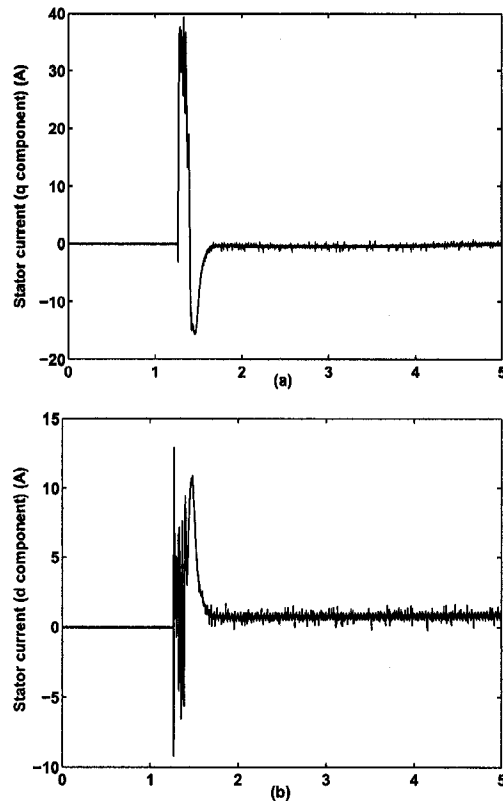


Figure 4.1: Errors of stator current (a) q component (b) d component

4.2 Unknown Input Observers

4.2.1 Theory of Unknown Input Observers

Conventional Luenberger observer assumes all inputs are known and measurable. However, in practice, there are many situations where some of system inputs are unmeasurable. In those cases the conventional observer may not work and an unknown input observer is a good choice. The basic principle of the unknown input observer is to decouple the unknown input terms from the known ones. In the applications of UIO for fault detection, by properly choosing the observer matrices, one can generate a residual, in which the effect of unknown inputs is decoupled from the state estimation errors caused by faults. This residual can then be used as the indication of faults. This is the idea behind the so-called robust fault detection.

Many approaches for designing unknown input observers have been proposed after the work of Wang et al. Fairman et al. [54] proposed the singular value decomposition method. Park and Stein [55] studied the simultaneous estimation problem for both states and unknown inputs. Chen, Patton, and Zhang [22] designed a full-order UIO and successfully applied it to a jet engine system. In their paper, they presented a rigorous mathematical foundation in designing a full-order UIO. The necessary and sufficient conditions for the existence of the UIO are given and thoroughly proved. We adopt the linear UIO technique, and extend it to nonlinear systems, especially to the induction motor system for the purpose of fault detection.

Consider a system with additive uncertainties (unknown inputs) described by the following equations:

$$\begin{aligned}\dot{x}(t) &= Ax(t) + Bu(t) + E_d d(t) \\ y(t) &= Cx(t)\end{aligned}\tag{4.21}$$

where $x(t) \in R^n$ is the state vector, $y(t) \in R^m$ is the output vector, $u(t) \in R^p$ is the input vector, and $d(t) \in R^q$ is a time-varying vector representing the unknown inputs (disturbances). $E_d \in R^{n \times q}$ is the distribution matrix representing the structure of the unknown inputs. Note that matrices A, B and C correspond to the state space description of a linear, time invariant system.

A full-order observer for system (4.21) is constructed as follows:

$$\begin{aligned}\dot{z}(t) &= Fz(t) + TBu(t) + Ky(t) \\ \hat{x}(t) &= z(t) + Hy(t)\end{aligned}\tag{4.22}$$

where $\hat{x}(t) \in R^n$ is the estimated state vector, $z(t) \in R^n$ is the state vector of the full-order unknown input observer, and F, T, K, H are matrices to be designed to decouple the effect of the unknown input from the estimation error. The observer described by (4.22) is illustrated in Figure 4.2.

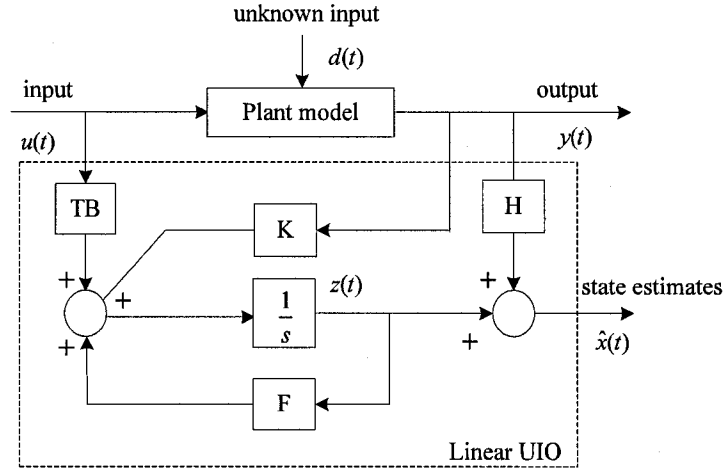


Figure 4.2: A full-order linear unknown input observer

By applying observer (4.22) to system (4.21), the state estimation error $e(t) = x(t) - \hat{x}(t)$ is governed by the following equation:

$$\begin{aligned}
 \dot{e}(t) &= \dot{x}(t) - \dot{\hat{x}}(t) \\
 &= Ax(t) + Bu(t) + E_d d(t) - \dot{z}(t) - H\dot{y}(t) \\
 &= Ax(t) + Bu(t) + E_d d(t) - Fz(t) - TBu(t) \\
 &\quad - (K_1 + K_2)y(t) - HC[Ax(t) + Bu(t) + E_d d(t)] \\
 &= (A - HCA - K_1C)x(t) - Fz(t) - K_2y(t) \\
 &\quad + [(I - HC) - T]Bu(t) + (I - HC)E_d d(t) \\
 &= (A - HCA - K_1C)e(t) + [(A - HCA - K_1C) - F]z(t) \\
 &\quad + [(A - HCA - K_1C)H - K_2]y(t) \\
 &\quad + [(I - HC) - T]Bu(t) + (I - HC)E_d d(t)
 \end{aligned}$$

where $K = K_1 + K_2$. By definition, an observer is called an unknown input observer for system (4.21), if its state estimation error vector approaches zero asymptotically regardless of the presence of the unknown input (disturbance) in the system, [22]. For (4.22) to be an unknown input observer for the system

(4.21), the following relationships must hold for matrices F , T , K , and H .

$$(I - HC)E_d = 0 \quad (4.23)$$

$$T = I - HC \quad (4.24)$$

$$F = A - HCA - K_1C \quad (4.25)$$

$$K_2 = FH \quad (4.26)$$

Given above relationships, the state estimation error reduces to:

$$\dot{e}(t) = Fe(t) \quad (4.27)$$

By selecting a stable matrix F (i.e., all eigenvalues are in the left half plane), $e(t)$ will be made to approach zero asymptotically despite of the disturbances. According to the definition, (4.22) is an UIO of (4.21). The design of the UIO involves, first of all, selecting a stable matrix F and then solving equations (4.23) - (4.26).

It has to be pointed out that an UIO may not exist for a linear system described by (4.21). The next theorem gives the necessary and sufficient conditions for (4.22) to be an UIO of (4.21).

Theorem 4.1: Necessary and sufficient conditions for (4.22) to be an UIO for the system defined by (4.21) are:

$$(i) \quad \text{rank}(CE_d) = \text{rank}(E_d)$$

$$(ii) \quad (C, A_1) \text{ is detectable,}$$

$$\text{where } A_1 = A - HCA$$

The proof can be found in [22].

Remark 1 The disturbance matrix E_d is assumed to have full column rank. If not, the following rank decomposition can be applied to matrix E_d :

$$E_d d(t) = E_1 E_2 d(t)$$

where E_1 is a full column rank matrix and $E_2d(t)$ can be considered as a new unknown input.

Remark 2 Condition (i) ensures that equation (4.23) is solvable for H . In [22], a special solution of H was given as $H = [(CE)^TCE]^{-1}(CE)^T$. To satisfy condition (i), the number of independent rows of matrix C must not be less than the number of the independent columns of the matrix E_d . This means that the maximum number of disturbances that are decoupled can not be larger than the number of the independent measurements, $y(t)$. Condition (ii) ensures that $F = A_1 - K_1C$ can be made Hurwitz by properly designing K_1 .

Remark 3 The matrix K_1 , which can be chosen to obtain a stable matrix F , is not unique. This design freedom can be exploited for other design objectives, for example, to make the residual have directional properties that can be utilized to fulfil the fault isolation task [22].

4.2.2 Design of An Unknown Input Observer for Fault Detection of Induction Motors

Consider induction motor nonlinear model described by (3.22). Also consider a disturbance ΔT_L acting on the nominal load torque T_L , and the actual load torque becomes $T_L + \Delta T_L$. In addition, we consider stator and rotor faults resulting in abrupt changes in stator and rotor resistance, as described in section 3.5. Then the induction motor with these faults and load disturbance can be described as follows:

$$\dot{x}(t) = Ax(t) + Bu(t) + f_a(x(t)) + E_d d(t) + E_f f(t) \quad (4.28)$$

$$y(t) = Cx(t) \quad (4.29)$$

where

$$A = \begin{bmatrix} -\gamma & -\omega_s & \alpha\beta & 0 & 0 \\ \omega_s & -\gamma & 0 & \alpha\beta & 0 \\ \alpha L_m & 0 & -\alpha & -\omega_s & 0 \\ 0 & \alpha L_m & \omega_s & -\alpha & 0 \\ 0 & 0 & 0 & 0 & \epsilon \end{bmatrix}$$

Matrix A contains the coefficients of the linear terms. A small value ϵ is introduced here to make matrix A full rank. Matrices B and C are same as in (3.22). The vector $f_a(x(t))$, which contains all the nonlinear terms of the motor model is shown as follows:

$$f_a(x) = \begin{bmatrix} -n_p\beta x_5 x_4 \\ n_p\beta x_5 x_3 \\ n_p\beta x_5 x_4 \\ -n_p\beta x_5 x_3 \\ \mu(x_4 x_1 - x_2 x_3) + \frac{T_L}{J} - \epsilon x_5 \end{bmatrix}$$

$E_{ad}(t)$ and $E_{ff}(t)$ are vectors caused by load disturbance and faults, respectively.

$$E_{ad}(t) = \begin{bmatrix} 0 \\ 0 \\ 0 \\ 0 \\ \frac{1}{J} \end{bmatrix} \cdot \Delta T_L$$

$$\begin{aligned} E_{ff}(t) &= \begin{bmatrix} -\frac{1}{\sigma L_s} x_1 \Delta R_s - \frac{L_m^2}{\sigma L_s L_r^2} x_1 \Delta R_r + \frac{\beta}{L_r} x_3 \Delta R_r \\ -\frac{1}{\sigma L_s} x_2 \Delta R_s - \frac{L_m^2}{\sigma L_s L_r^2} x_2 \Delta R_r + \frac{\beta}{L_r} x_4 \Delta R_r \\ \frac{L_m}{L_r} x_1 \Delta R_r - \frac{1}{L_r} x_3 \Delta R_r \\ \frac{L_m}{L_r} x_2 \Delta R_r - \frac{1}{L_r} x_4 \Delta R_r \\ 0 \end{bmatrix} \\ &= \begin{bmatrix} -\frac{1}{\sigma L_s} & -\frac{L_m^2}{\sigma L_s L_r^2} & 0 & 0 & 0 & \frac{\beta}{L_r} & 0 & 0 \\ 0 & 0 & -\frac{1}{\sigma L_s} & -\frac{L_m^2}{\sigma L_s L_r^2} & 0 & 0 & 0 & \frac{\beta}{L_r} \\ 0 & \frac{L_m}{L_r} & 0 & 0 & 0 & -\frac{1}{L_r} & 0 & 0 \\ 0 & 0 & 0 & \frac{L_m}{L_r} & 0 & 0 & 0 & -\frac{1}{L_r} \\ 0 & 0 & 0 & 0 & 0 & 0 & 0 & 0 \end{bmatrix} \cdot \begin{bmatrix} x_1 \Delta R_s \\ x_1 \Delta R_r \\ x_2 \Delta R_s \\ x_2 \Delta R_r \\ x_3 \Delta R_s \\ x_3 \Delta R_r \\ x_4 \Delta R_s \\ x_4 \Delta R_r \end{bmatrix} \end{aligned}$$

where $d(t) = \Delta T_L$ is load disturbance and $f(t) = [x_1 \Delta R_s \quad x_1 \Delta R_r \quad x_2 \Delta R_s \quad x_2 \Delta R_r \quad x_3 \Delta R_s \quad x_3 \Delta R_r \quad x_4 \Delta R_s \quad x_4 \Delta R_r]^T$ the fault induced vector.

A full-order observer is constructed as

$$\begin{aligned}\dot{z}(t) &= T f_a(\hat{x}(t)) + Fz(t) + TBu(t) + Ky(t) \\ \hat{x}(t) &= z(t) + Hy(t)\end{aligned}\quad (4.30)$$

Here we adopt the structure of linear UIO, but insert additional nonlinear terms in the observer dynamics. The state estimation error is shown to be:

$$\begin{aligned}\dot{e}(t) &= \dot{x}(t) - \dot{\hat{x}}(t) \\ &= Ax(t) + Bu(t) + f_a(x(t)) + E_d d(t) + E_f f(t) - \dot{z}(t) - H\dot{y}(t) \\ &= Ax(t) + Bu(t) + f_a(x(t)) + E_d d(t) + E_f f(t) \\ &\quad - T f_a(\hat{x}(t)) - Fz(t) - TBu(t) - (K_1 + K_2)y(t) \\ &\quad - HC[Ax(t) + Bu(t) + f_a(x(t)) + E_d d(t) + E_f f(t)] \\ &= (A - HCA - K_1 C)e(t) + [(I - HC)f_a(x(t)) - T f_a(\hat{x}(t))] \\ &\quad + [(A - HCA - K_1 C) - F]z(t) \\ &\quad + [(A - HCA - K_1 C)H - K_2]y(t) \\ &\quad + [(I - HC) - T]Bu(t) \\ &\quad + (I - HC)E_d d(t) \\ &\quad + (I - HC)E_f f(t)\end{aligned}\quad (4.31)$$

where $K = K_1 + K_2$. As in linear case, if the equations (4.23) to (4.26) are true, the state estimation error reduces to

$$\dot{e}(t) = Fe(t) + T[f_a(x(t)) - f_a(\hat{x}(t))] + TE_d d(t) + TE_f f(t)$$

If we linearize the nonlinear term $f_a(x(t))$ in the neighborhood of the estimated state, we have

$$\begin{aligned}\dot{e}(t) &= Fe(t) + T \frac{\partial f_a(x(t))}{\partial x(t)} \Big|_{x(t)=\hat{x}(t)} e(t) + TE_d d(t) + TE_f f(t) \\ &= Fe(t) + T \Delta A \{\hat{x}(t)\} e(t) + TE_d d(t) + TE_f f(t)\end{aligned}$$

where

$$\begin{aligned} \Delta A\{\hat{x}(t)\} &= \frac{\partial f_a(x(t))}{\partial x(t)} \Big|_{x(t)=\hat{x}(t)} \\ &= \begin{bmatrix} 0 & 0 & 0 & -n_p\beta\hat{x}_5(t) & -n_p\beta\hat{x}_4(t) \\ 0 & 0 & n_p\beta\hat{x}_5(t) & 0 & n_p\beta\hat{x}_3(t) \\ 0 & 0 & 0 & n_p\hat{x}_5(t) & n_p\hat{x}_4(t) \\ 0 & 0 & -n_p\hat{x}_5(t) & 0 & -n_p\hat{x}_3(t) \\ \mu\hat{x}_4 & -\mu\hat{x}_3 & -\mu\hat{x}_2 & \mu\hat{x}_1 & -\epsilon \end{bmatrix} \end{aligned}$$

At this point, we rewrite the state estimation error as

$$\dot{e}(t) = (F + T\Delta A\{\hat{x}(t)\})e(t) + TE_d d(t) + TE_f f(t) \quad (4.32)$$

The objective is to design H , T , F , K_1 and K_2 , such that the following relations hold:

$$(I - HC)E_d = 0 \quad (4.33)$$

$$(I - HC)E_f \neq 0 \quad (4.34)$$

$$T = I - HC \quad (4.35)$$

$$F = A - HCA - K_1C \quad (4.36)$$

$$F + T\Delta A\{\hat{x}(t)\} \text{ is Hurwitz} \quad (4.37)$$

$$K_2 = FH \quad (4.38)$$

Then (4.27) becomes:

$$\dot{e}(t) = (F + T\Delta A\{\hat{x}(t)\})e(t) + TE_f f(t) \quad (4.39)$$

Compared to (4.27), (4.39) has two extra terms, $\Delta A\{\hat{x}(t)\}$ and $E_f f(t)$. The former is resulted from the nonlinear part $f_a(x)$ in the model and the latter is from the faults. Since $F + T\Delta A\{\hat{x}(t)\}$ can be made Hurwitz by designing K_1 properly, $e(t)$ will be independent of the disturbance and be affected by the faults only.

The structure of the designed UIO for induction motor is illustrated in figure 4.3. It has a similar structure as linear UIO. The difference is the nonlinear

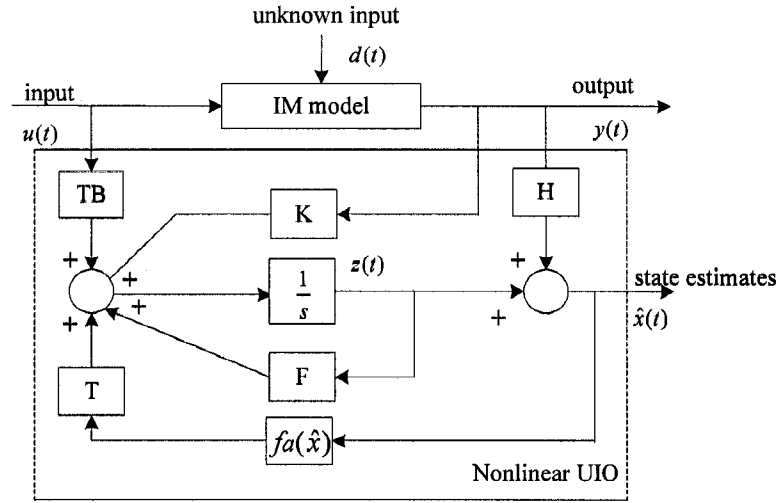


Figure 4.3: A full-order unknown input observer for induction motors

term in the induction motor model is inserted in the observer dynamics.

The design procedure is as follows:

1. Choose T and compute H

The matrix H satisfying (4.33) and (4.34) is not unique and thus is matrix T . In paper [53], the authors have concluded the conditions under which (4.33) is solvable and have given a special solution of H . They did not include condition (4.34), and the fault detection was achieved by using the design freedom of matrix K_1 . Because of the structure of the induction motor model and the considered faults, the matrix H can not be calculated the way as in [53]. Otherwise the effect of both faults and disturbances on the estimation error will be eliminated, thus the faults can not be detected. Here we first choose T based on the following considerations:

- (1) $TE_d = 0$
- (2) $TE_f \neq 0$
- (3) H is solvable from (4.35).
- (4) Choose T such that the eigenvalues of $F + T\Delta A\{\hat{x}(t)\}$ are only a function of \hat{x}_5 , the estimated motor speed, and are independent of the rest of

state estimates. This could be achieved by considering the specific structure of $\Delta A\{\hat{x}(t)\}$. By doing so, a constant matrix K_1 can be used to make (4.39) stable.

Based on above considerations, the matrix T is chosen as

$$T = \begin{bmatrix} 1 & 0 & 0 & 0 & 0 \\ 0 & 1 & 0 & 0 & 0 \\ \frac{1}{\beta} & 0 & 1 & 0 & 0 \\ 0 & \frac{1}{\beta} & 0 & 1 & 0 \\ 0 & 0 & 0 & 0 & 0 \end{bmatrix}$$

Then H is computed from (4.35) as

$$H = \begin{bmatrix} 0 & 0 & 0 \\ 0 & 0 & 0 \\ -\frac{1}{\beta} & 0 & 0 \\ 0 & -\frac{1}{\beta} & 0 \\ 0 & 0 & 1 \end{bmatrix}$$

and

$$A_1 = A - HCA = TA$$

$$= \begin{bmatrix} -\gamma & -\omega_s & \alpha\beta & 0 & 0 \\ \omega_s & -\gamma & 0 & \alpha\beta & 0 \\ -\frac{\gamma}{\beta} + \alpha L_m & -\frac{\omega_s}{\beta} & 0 & -\omega_s & 0 \\ \frac{\omega_s}{\beta} & -\frac{\gamma}{\beta} + \alpha L_m & \omega_s & 0 & 0 \\ 0 & 0 & 0 & 0 & 0 \end{bmatrix}$$

$$T\Delta A\{\hat{x}(t)\} = \begin{bmatrix} 0 & 0 & 0 & -n_p\beta\hat{x}_5 & -n_p\beta\hat{x}_4 \\ 0 & 0 & n_p\beta\hat{x}_5 & 0 & n_p\beta\hat{x}_3 \\ 0 & 0 & 0 & 0 & 0 \\ 0 & 0 & 0 & 0 & 0 \\ 0 & 0 & 0 & 0 & 0 \end{bmatrix}$$

Notice that all elements in the last row of T are zeros. In this case, the speed estimation error $x_5 - \hat{x}_5$ only depends on F from (4.39) in normal operations

and it will converge to zero as long as F has all stable eigenvalues. Due to this fact, $T\Delta A\{\hat{x}(t)\}$ can be written as the following by replacing \hat{x}_5 with ω :

$$T\Delta A\{\hat{x}(t)\} = \begin{bmatrix} 0 & 0 & 0 & -n_p\beta\omega & -n_p\beta\hat{x}_4 \\ 0 & 0 & n_p\beta\omega & 0 & n_p\beta\hat{x}_3 \\ 0 & 0 & 0 & 0 & 0 \\ 0 & 0 & 0 & 0 & 0 \\ 0 & 0 & 0 & 0 & 0 \end{bmatrix}$$

2. Check whether the following existing conditions are satisfied

- (i) $\text{rank}(CE_d) = \text{rank}(E_d)$
- (ii) (C, A_1) is detectable, where $A_1 = A - HCA$

From induction motor model (4.28) - (4.29),

$$\text{rank}(CE_d) = \text{rank}(E_d) = 1$$

$$\text{rank} \begin{pmatrix} C \\ CA_1 \\ CA_1^2 \\ CA_1^3 \\ CA_1^4 \end{pmatrix} = 5 \implies (C, A_1) \text{ is detectable,}$$

Hence there exists an UIO for induction motor model described by (4.29).

3. Design K_1 such that $\bar{F} = A_1 + T\Delta A\{\hat{x}(t)\} - K_1C$ is Hurwitz

Denote

$$\begin{aligned} \bar{A} &= A_1 + T\Delta A\{\hat{x}(t)\} \\ &= \begin{bmatrix} -\gamma & -\omega_s & \alpha\beta & -n_p\beta\omega & -n_p\beta\hat{x}_4 \\ \omega_s & -\gamma & n_p\beta\omega & \alpha\beta & n_p\beta\hat{x}_3 \\ -\frac{\gamma}{\beta} + \alpha L_m & -\frac{\omega_s}{\beta} & 0 & -\omega_s & 0 \\ \frac{\omega_s}{\beta} & -\frac{\gamma}{\beta} + \alpha L_m & \omega_s & 0 & 0 \\ 0 & 0 & 0 & 0 & 0 \end{bmatrix} \\ &= \begin{bmatrix} \bar{A}_{11} & \bar{A}_{12} \\ 0 & 0 \end{bmatrix} \end{aligned}$$

where

$$\bar{A}_{11} = \begin{bmatrix} -\gamma & -\omega_s & \alpha\beta & -n_p\beta\omega \\ \omega_s & -\gamma & n_p\beta\omega & \alpha\beta \\ -\frac{\gamma}{\beta} + \alpha L_m & -\frac{\omega_s}{\beta} & 0 & -\omega_s \\ \frac{\omega_s}{\beta} & -\frac{\gamma}{\beta} + \alpha L_m & \omega_s & 0 \end{bmatrix}$$

$$\bar{A}_{12} = \begin{bmatrix} -n_p\beta\hat{x}_4 \\ n_p\beta\hat{x}_3 \\ 0 \\ 0 \end{bmatrix}$$

Partition C as:

$$C = \begin{bmatrix} C_{11} & 0 \\ 0 & C_{22} \end{bmatrix}, \quad \text{where} \quad C_{11} = \begin{bmatrix} 1 & 0 & 0 & 0 \\ 0 & 1 & 0 & 0 \end{bmatrix}, \quad C_{22} = 1$$

Let K_1 have the following form:

$$K_1 = \begin{bmatrix} K_{11} & K_{12} \\ 0 & K_{22} \end{bmatrix}$$

Then

$$\begin{aligned} \bar{F} &= A_1 + T\Delta A\{\hat{x}(t)\} - K_1C \\ &= \bar{A} - K_1C \\ &= \begin{bmatrix} \bar{A}_{11} & \bar{A}_{12} \\ 0 & 0 \end{bmatrix} - \begin{bmatrix} K_{11} & K_{12} \\ 0 & K_{22} \end{bmatrix} \begin{bmatrix} C_{11} & 0 \\ 0 & C_{22} \end{bmatrix} \\ &= \begin{bmatrix} \bar{A}_{11} - K_{11}C_{11} & \bar{A}_{12} - K_{12} \\ 0 & -K_{22} \end{bmatrix} \end{aligned} \quad (4.40)$$

It follows that the states estimates \hat{x}_3 and \hat{x}_4 do not affect the eigenvalues of F. Denote $F_{11} = \bar{A}_{11} - K_{11}C_{11}$. Since (C_{11}, A_{11}) is detectable, F_{11} can be made Hurwitz by choosing K_{11} . In fact, following the similar procedure as in bilinear

observer stability analysis in Section 4.1.3, the stability of the observer error dynamics in (4.39) can be verified. K_{11} can be designed using pole placement and K_{22} is selected as a positive number.

4. Compute matrices F , K_2 , and K

After T , H and K_1 are determined, F , K_2 and thus K can be finally computed as:

$$F = A - HCA - K_1C$$

$$K_2 = FH$$

$$K = K_1 + K_2$$

Following the above design procedure, an unknown input observer is designed for the induction motor used in Section 3.4. By substituting the parameters in Table 3.1 in the motor model, the observer gains are obtained by placing poles of (4.39) at $[-20 \ -20 \ -50 \ -50 \ -20]$ as follows:

$$K_1 = \begin{bmatrix} -277.3021 & -753.9822 & 0 \\ 753.9822 & -277.3021 & 0 \\ -2.7773 & -13.0618 & 0 \\ 13.0618 & -2.7773 & 0 \\ 0 & 0 & 20 \end{bmatrix}, \quad F = \begin{bmatrix} -700 & 377 & 1.258 & 0 & 0 \\ -377 & 700 & 0 & 1258 & 0 \\ -0.8 & 6.7 & 0 & -377 & 0 \\ -6.7 & -0.8 & 377 & 0 & 0 \\ 0 & 0 & 0 & 0 & -20 \end{bmatrix}$$

$$K_2 = \begin{bmatrix} -21.1640 & 0 & 0 \\ 0 & -21.1640 & 0 \\ 0 & 6.3424 & 0 \\ -6.3424 & 0 & 0 \\ 0 & 0 & -20 \end{bmatrix}, \quad K = \begin{bmatrix} -298.4671 & -753.9822 & 0 \\ 753.9822 & -298.4661 & 0 \\ -2.7773 & -6.7194 & 0 \\ 6.7194 & -2.7773 & 0 \\ 0 & 0 & 0 \end{bmatrix}$$

Remark In Section 4.1, a bilinear observer is introduced but without considering robustness to the disturbances. However, it is possible to apply the concept and conditions of an unknown input observer to the induction motor bilinear model. In another word, one can design a robust bilinear observer base FD for induction motors. This would be left as one of the future work.

Chapter 5

Implementation of Induction Motor Fault Detection

In this chapter, a real-time simulation of the observer-based fault detection schemes for an induction motor using RT-Lab software is presented. Satisfactory results are obtained with a fixed time-step of $100 \mu\text{s}$. The chapter starts with the RT-Lab implementation of the observers, and a variety of simulation results under different scenarios are provided. It follows that the designed bilinear observer and unknown input observer are robust to load disturbance and power supply imbalance.

5.1 RT-Lab Real-time Simulation Software

The designed bilinear observer and unknown input observer have been implemented using RT-Lab software package, as shown in figure 5.1.

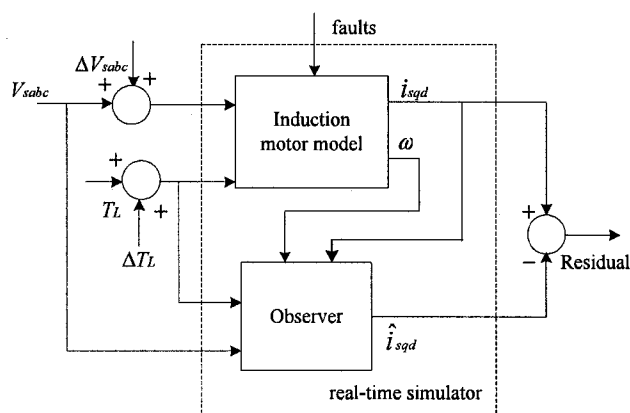


Figure 5.1: RT-Lab simulation

RT-Lab is an industrial-grade software for engineers who use mathematical block diagrams for simulation, control, and related applications. It uses the popular Matlab/Simulink for editing and viewing graphic models in block-diagram format. The block diagrams made with Matlab/Simulink can be used by RT-Lab to generate necessary code for real-time simulations on a single or more target processors. However, Matlab/Simulink block diagrams have to be separated into subsystems and inserted appropriate communication blocks

before they are executed by RT-Lab.

RT-Lab recognizes three types of subsystems [31]: (1) Console subsystem, which is the station operating under Windows XP, where the user interacts with the system. It contains all the Matlab/Simulink blocks related to acquiring and viewing data. (2) Master subsystem, which is responsible for the model's real-time calculation and for the overall synchronization of the network. There can be only one master subsystem in one model. (3) Slave subsystem is also responsible for performing calculations in the model and is driven by the master subsystem. A model may contain several slave subsystems.

Once the model is grouped into console and computation subsystems, special blocks called OpComm blocks must be inserted into the subsystems. In RT-Lab, a computation subsystem waits for reception of all signals before it is able to start calculation. OpComm blocks are used to intercept all incoming signals before sending them to computation blocks within a given subsystem.

The system given in Fig. 5.1 is implemented in RTX-Lab as in Fig. 5.2 and Fig. 5.3. It is distributed over two target nodes. The first node, acting as master subsystem (SM-IM Model), computes the induction motor model in real-time; the second one, acting as slave subsystem (SS-Observer), computes in real-time the observer. SC-User-Interface is the console. It contains the input signals, manual switches, and signal visualization.

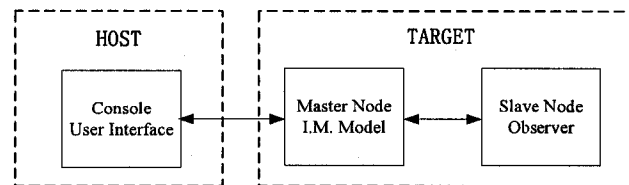


Figure 5.2: RTX-Lab simulation diagram

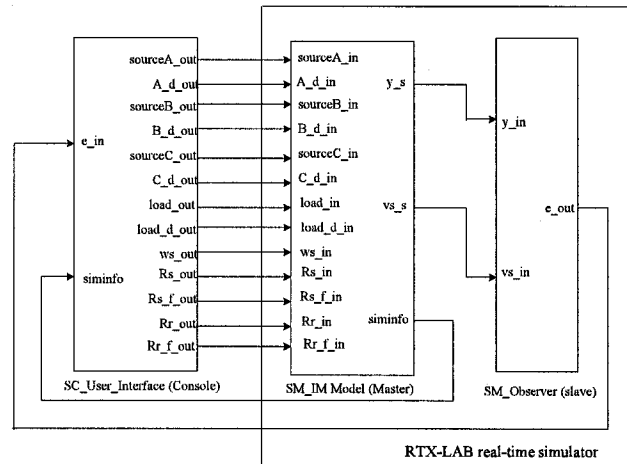


Figure 5.3: RT-Lab graphic model of observer-based IM fault detection

5.2 Real-time Simulation Results

RT-Lab requires that the time factor equal to 1 in order to get accurate results. By testing, a step size of $100\mu\text{s}$ is chosen, which results no overrun with a time factor of 1. Two types of disturbances are considered: 1) A load torque of -5 N.m is disturbed by step changes. 2) The magnitude of the stator phase A voltage is increased by 10%, making the three phase input voltage unbalanced. We also consider two types of faults: stator shorted winding turns and broken rotor bars, which result in abrupt changes in stator resistance and rotor resistance, respectively. The considered disturbances and faults are shown in Figure 5.4.

The observers were simulated in the following cases:

- Case 1** No faults but two types of disturbances present
- Case 2** Rotor fault without disturbances
- Case 3** Stator fault without disturbances
- Case 4** Rotor fault with two types of disturbances present.
- Case 5** Stator fault with two types of disturbances present.

It was pointed out that two of the bilinear observer poles are assignable and

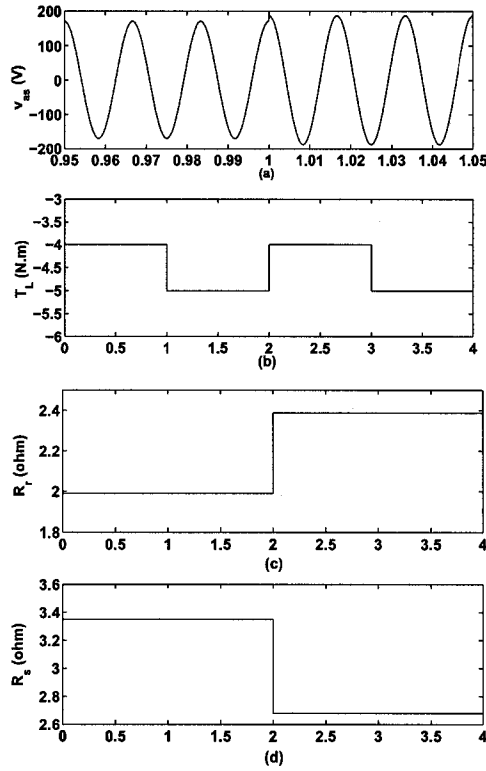


Figure 5.4: Disturbance and fault signals used in simulation (a) Stator phase A voltage (b) Load torque (c) Rotor resistance (d) Stator resistance

the other two are not but located on the left-half of s-plane. In the simulation, the two assignable eigenvalues are placed at $[-100 -100]$. For the UIO, the poles are placed at $[-20 -20 -50 -50 -20]$. Since the rotor fluxes are not measurable, we will use dq components of stator current for fault detection. Figure 5.5 - Figure 5.9 show the real-time simulation results of the BLO and UIO for the above five cases. Figure 5.5 shows that when there are no faults occurred, the estimation error of stator current (residual) converges to zero regardless of the presence of the disturbances, which is as expected. This means that the observers can estimate the current of a healthy motor. In Figure 5.6 - 5.9, where rotor and stator faults occurred, the observers captured the abrupt changes in the resistance, producing nonzero residual. Note that, for the bi-linear observer, the error of motor speed diverges even in normal conditions; on the other hand, for the unknown input observer, the error of motor speed stays to be zero despite of the faults. For this reason, the speed error can not

be used as residual.

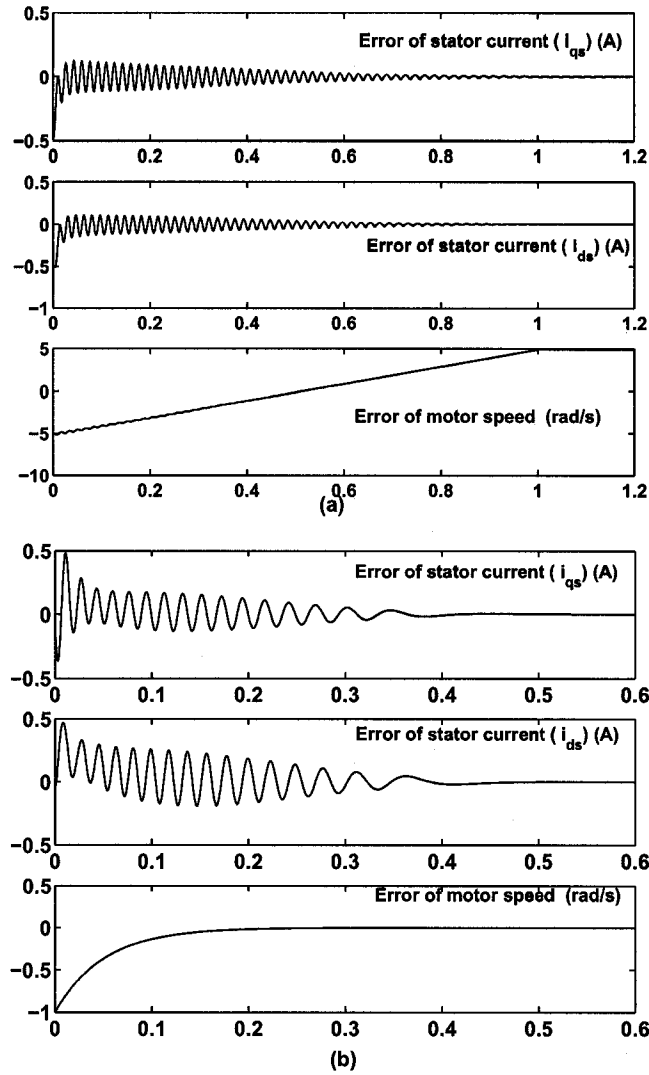


Figure 5.5: Estimation error of case 1, where there are no fault but the disturbances present (a) Bilinear observer: the errors of stator current go to zero regardless of the disturbances, but the speed error diverges. For this reason, the speed error of the BLO can not be used as residual signal. (b) Unknown input observer: The estimation errors converge to zero regardless of the disturbances.

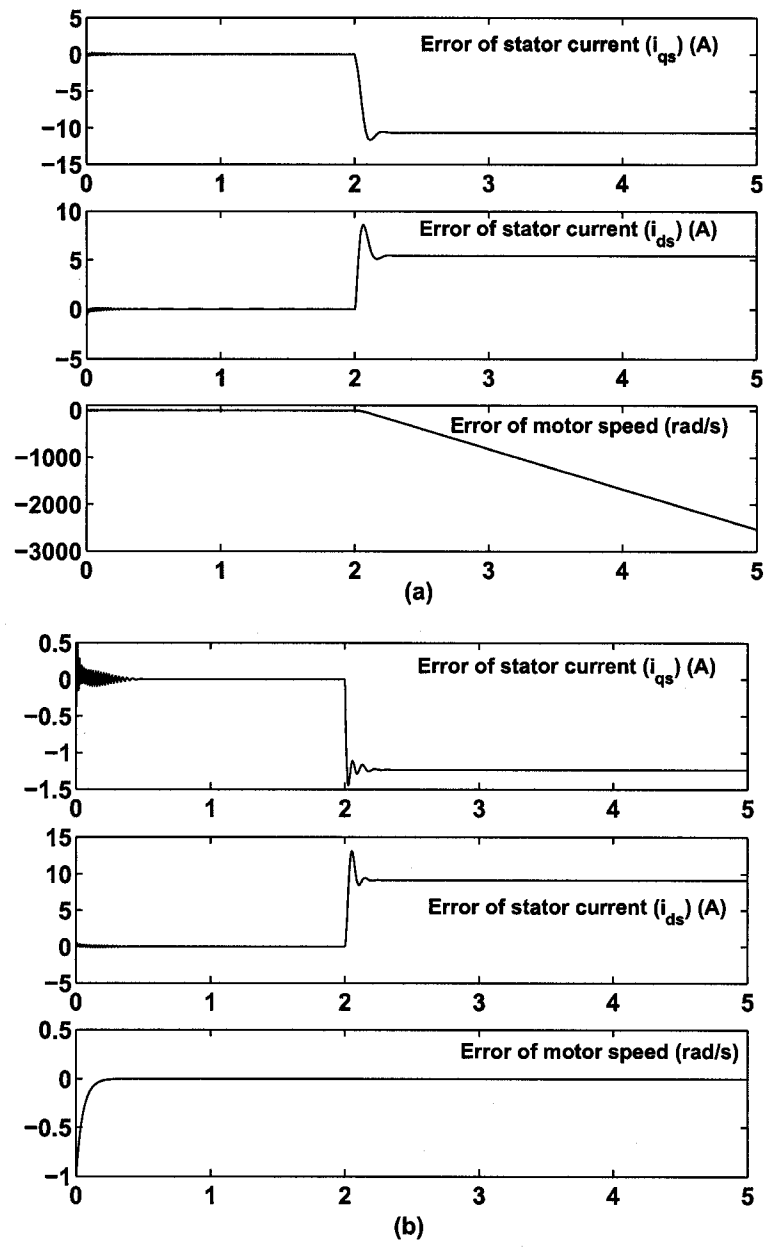


Figure 5.6: Estimation error of case 2, where rotor resistance increased by 20% at $t = 2$ second. The observers captured the fault and the error of stator currents become nonzero at the time fault occurred. (a) Bilinear observer: the speed error diverges (b) Unknown input observer: the speed error is zero despite of the fault. For this reason, the speed error of the UIO can not be used as residual signal.

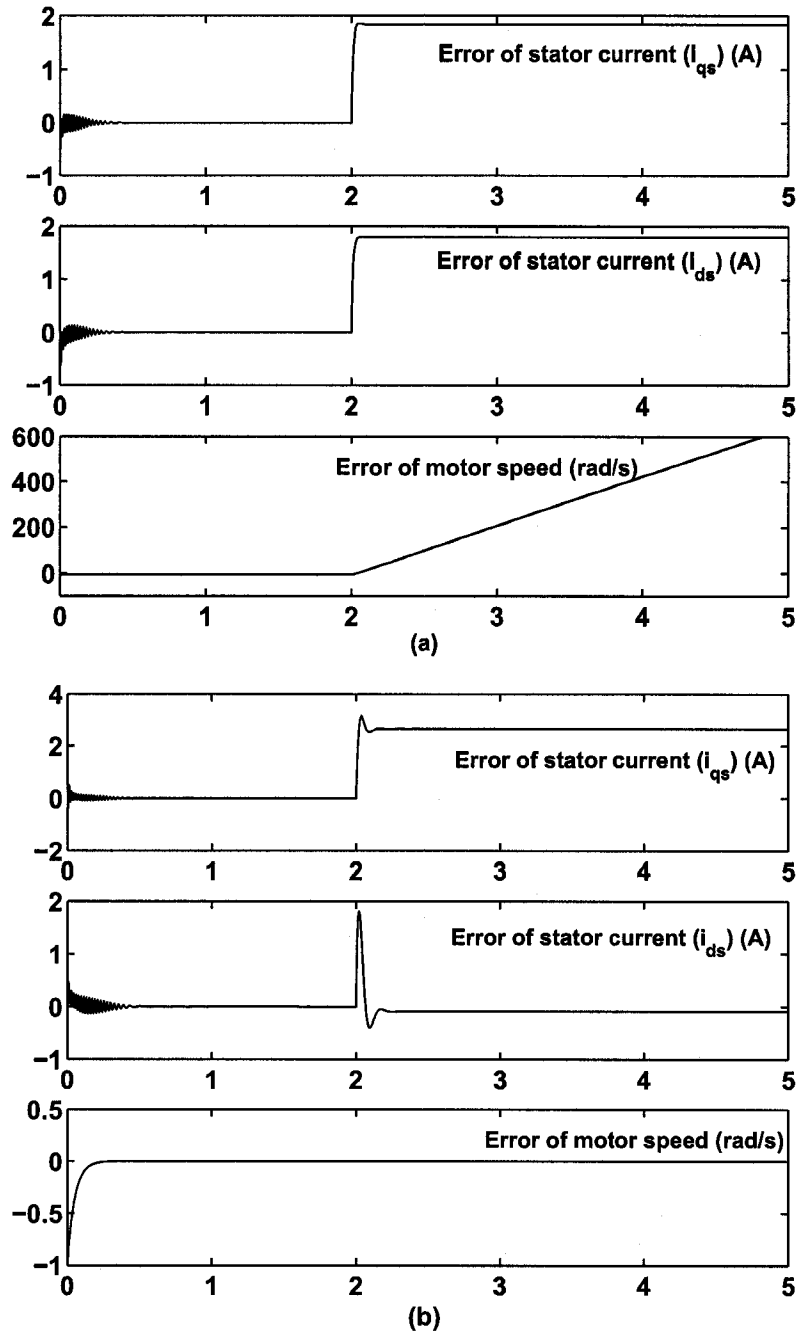


Figure 5.7: Estimation error of case 3, where stator resistance increased by 20% at $t = 2$ second. The observers captured the fault and the error of stator currents become nonzero at the time fault occurred. (a) Bilinear observer: the speed error diverges (b) Unknown input observer: the speed error is zero despite of the fault.

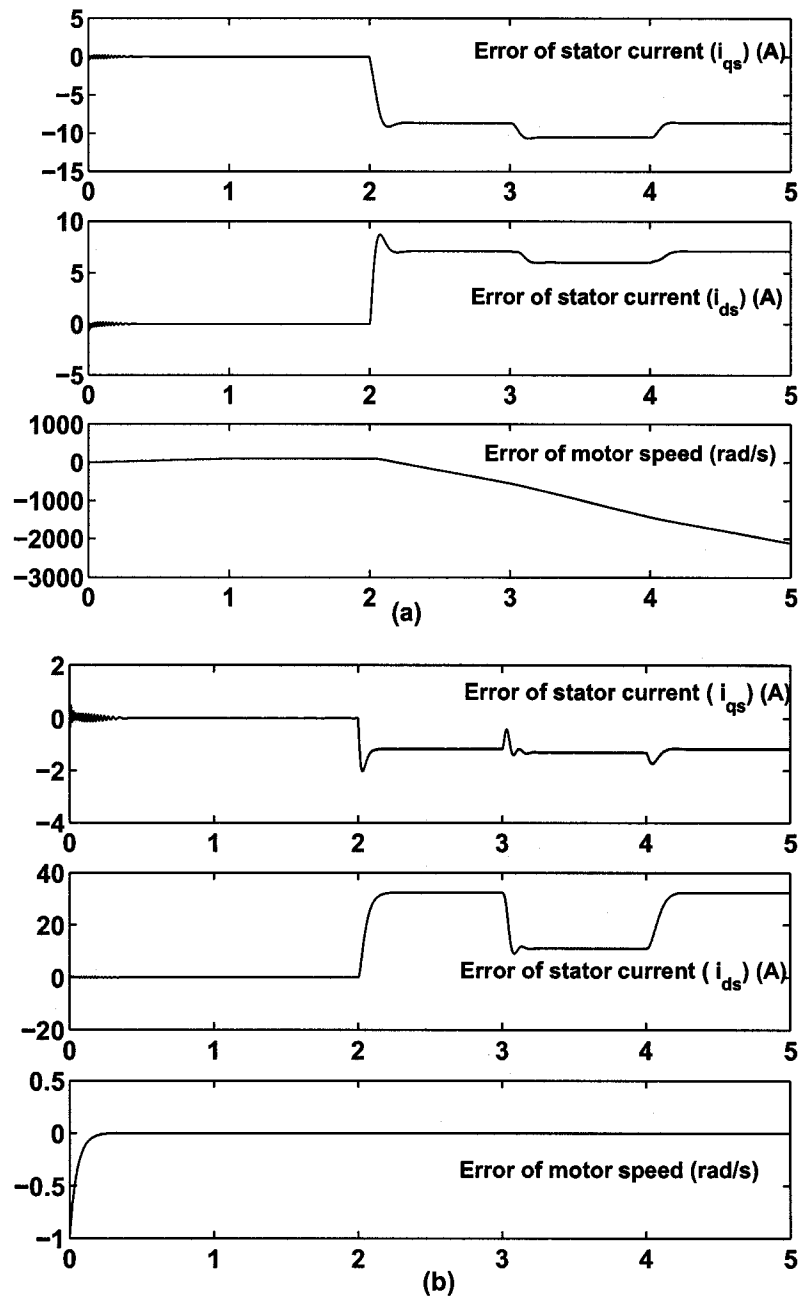


Figure 5.8: Estimation error of case 4, where the rotor resistance increased by 20% at $t = 2$ second with two types of disturbances present. The estimation errors of stator current become nonzero at the time fault occurred, thus the fault is detected. (a) Bilinear observer: speed error diverges (b) Unknown input observer: the speed error stays to be zero despite of the fault.

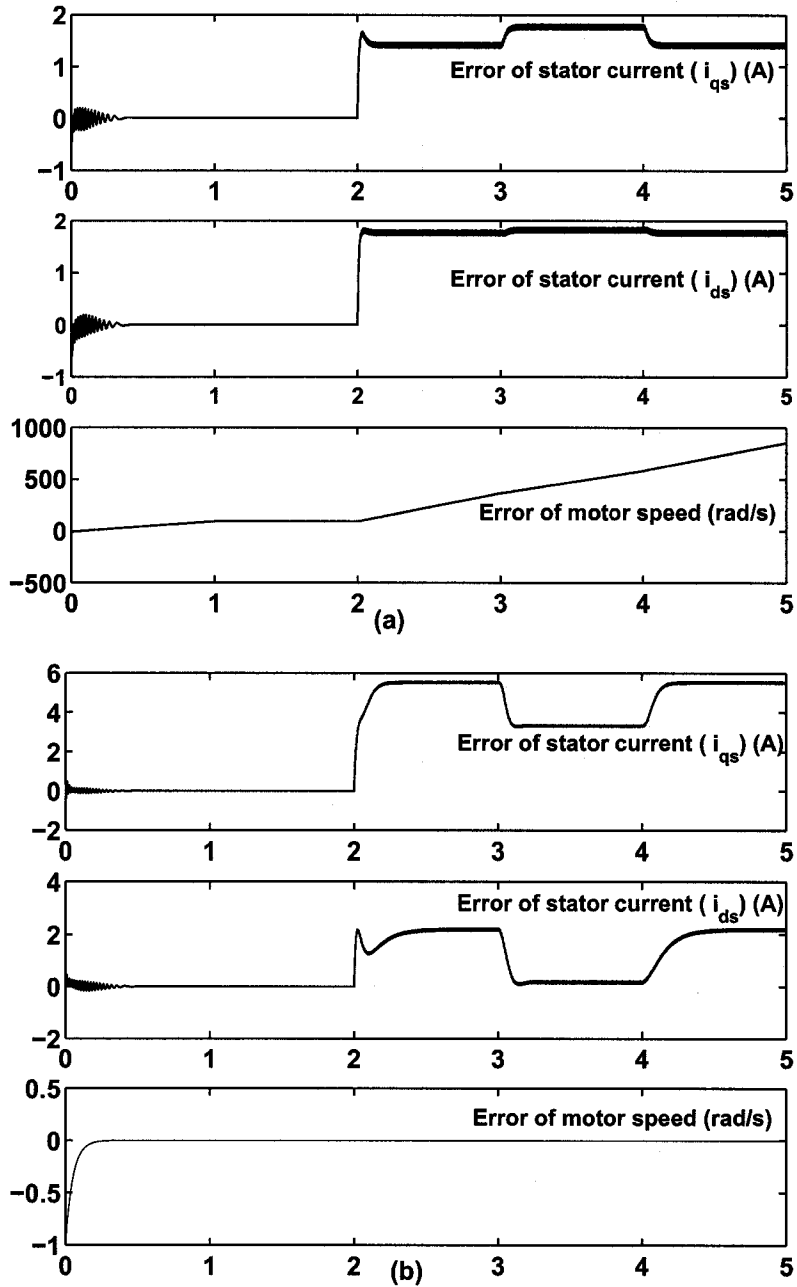


Figure 5.9: Estimation error of case 5, where the stator fault happened at $t = 2$ second with two types of disturbances present. The estimation errors of stator current become nonzero at the time fault occurred, thus the fault is detected. (a) Bilinear observer: speed error diverges (b) Unknown input observer: the speed error stays to be zero despite of the fault.

Chapter 6

Conclusions

This thesis demonstrated how model-based, specifically, observer-based techniques could be applied to induction motor fault detection problem. This chapter concludes on the work presented in this thesis and gives recommendations for further work.

6.1 Conclusions

The following general conclusions can be drawn from the work in this thesis:

1. Model-based approach to fault detection in dynamic systems has been receiving more and more attention in recent years because of the development of the modern control theory. It is a good method for fault detection when the process model is known. However, it is seldom studied in the field of induction motor fault detection. Since the induction motor model is well-understood, it is worth to be studied.

2. The induction motor is originally modeled in its three-phase frame. However the model equations contain time-varying parameters because of the coupling between the mechanical part and electrical part. To eliminate these time-varying parameters, the equations are transformed to two-phase reference frames. Different reference frame has advantages for some purposes. We have shown that synchronously rotating frame is a good choice for induction motor fault detection, in which the state variables become constants in steady state.

3. The induction motor model has a strong bilinear structure if the motor speed is treated as a time-varying parameter, thus a bilinear observer is a good choice for estimating the states of a healthy motor. Two eigenvalues of the bilinear observer are not assignable. They are determined by the motor parameters and are located on the left-half of s-plane. However, negative eigenvalues can not guarantee the stability of a time-varying system. An analysis of the observer error dynamics shows that the stability can be guaranteed since

the motor speed is changing slowly.

4. Unknown input observers are ideal methods for systems with unknown inputs, and they have been well developed for linear systems. By considering the specific induction motor model, a fault detection unknown input observer, which makes use of the complete nonlinear model of the induction motor, is developed in this thesis. It is insensitive to the disturbances and sensitive to faults only. It is an extension of the linear unknown input observer. In the design, instead treating the nonlinearities as disturbances, which will increase the number of unknown inputs, they are incorporated into the system matrix of the error dynamics.

6.2 Recommendations for Further Work

The following topics would benefit from further work:

- **Robustness**

The designed observers are robust to load disturbance and power supply imbalance. However, the parameter variation is not considered. In fact, the rotor resistance depends on working conditions, and the rotor resistance will vary when the temperature varies. Generally speaking, model uncertainties can be treated as unknown input terms, but it is almost impossible to perfectly decouple them from the residual signal. In this case, one can use the optimization based fault detection method.

- **UIO for bilinear model**

It could be seen that the UIO design eventually leads to designing an observer for a bilinear subsystem. So it is possible to design an unknown input observer based on the induction motor bilinear model.

- **Hardware-in-the-Loop**

RT-Lab facilities real-time simulation with hardware-in-the-loop. A fu-

ture work could be done by including a real induction motor into real-time simulation via RT-Lab I/O boards to test the fault detection schemes.

Bibliography

- [1] M. P. Kaźmierkowski, and H. Tunia, Automatic control of converter-fed drives, *Polish Scientific Publishers PWN Ltd, Warszawa*.
- [2] S. Simani, C. Fantuzzi, and R. J. Patton, Model-based fault diagnosis in dynamic systems using identification techniques, *Springer*.
- [3] S. M. Bennett, R. J. Patton, S. Daley and D. A. Newton, Torque and flux estimation for a rail traction system in the presence of intermittent sensor faults, *UKACC International Conference on Control*, 2-5 September 1996.
- [4] F. Amato, M. Mattei, R. Iervolino, and G. Paviglianiti, A nonlinear UIO scheme for the FDI on a small commercial aircraft, *Proceedings of the 2002 IEEE International Conference on Control Applications* September 18-20, 2002 Glasgow, Scotland, U.K.
- [5] S. Williamson and K. Mirzoian, Analysis of cage induction motors with stator winding faults, *IEEE Trans. Power App. Syst.*, Vol 104, No.7, pp. 1838-1842, July 1985.
- [6] J. Sottile and J. L. Kohler, An online method to detect incipient failure of turn insulation in random wound motors, *IEEE Trans. Energy Conv.*, Vol 8, pp. 762-768, 1993.
- [7] G. B. Kliman, W. J. Premerlani, R. A. Koegl, and D. Hoeweler, A new approach to online turn fault detection in AC motors, *Proc. IEEE-IAS Annu. Meeting*, pp. 687-693, Oct. 1996.
- [8] R. R. Schoen, T. G. Habetler, F. Kamran, and R. G. Bartheld, Motor bearing damage detection using stator current monitoring, *IEEE Trans. Ind. Applicat.*, Vol. 31, pp. 1274-1279, Nov./Dec. 1995.
- [9] F. Filippetti, G. Franceschini, C. Tassoni, and P. Vas, AI techniques in induction machines diagnosis including the speed ripple effect, *IEEE Trans. Ind. Applicat.*, Vol. 34, pp. 98-108, Jan./Feb. 1998.
- [10] J. Penman and A. Stavrou, Broken rotor bars: Their effect on the transient performance of induction machines, *Proc. Inst. Elect. Eng. Electric Power Applications*, Vol. 143, No. 6, pp. 449-457, Nov. 1996.
- [11] Z. Ye and B. Wu, A review on induction motor online fault diagnosis, *Power Electronics and Motion Control Conference, Proceedings. PIEMC* Vol. 3, pp. 1353 - 1358, 15-18 Aug. 2000.

- [12] A. Wolfram, and R. Iserman, On-line fault detection of inverter-fed induction motors using advanced signal processing techniques, *Proceedings of the IFAC Safeprocess*, Budapest, Hungary, pp. 1151-1156, 2000.
- [13] B. Li, M. Y. Chow, Y. Tipsuwan and J.C. Hung, Neural network based motor rolling bearing fault diagnosis, *IEEE Trans. Indus. Electr*, Vol. 47, pp. 1060-1069, 2000.
- [14] S. Kolla and L. Varatharasa, Identifying three-phase induction motor faults using artificial neural networks, *ISA Transactions*, Vol. 39, issue 4, pp. 433-439, Sep. 2000.
- [15] K. Chris and L. Li, Induction motor fault detection and diagnosis using artificial neural networks Mechefske, *Proc. of the ASME International Design Engineering Technical Conferences and Computers and Information in Engineering Conferences - 20th Biennial Conf. on Mechanical Vibration and Noise*, pp. 543-550, 2005.
- [16] S. L. HO and K. M. Lau, Detection of faults in induction motors using artificial neural networks, *Proceedings of the 7th International Conference on Electrical Machines and Drives*, pp. 176-181 Sep 11-13 1995, Durham, UK
- [17] M. Rokonzaman and M. A. Rahman, Neural network based incipient fault detection of induction motors, *Proceedings of IEEE/IAS International Conference on Industrial Automation and Control*, pp. 199-202, 1995, Hyderabad, India.
- [18] M. Chow, R. Sharpe, and J. Huang, A methodology using fuzzy logic to optimize feed forward artificial neural network configurations, *IEEE Transactions, system, man and cybernetics*, Vol. 24, No. 5, pp. 760-768, 1994.
- [19] K. Watanabe and D. M. Himmelblau, Instrument fault detection in systems with uncertainties, *Int. J. System Sci.*, Vol. 13, No. 2, pp. 137-158, 1982.
- [20] R. J. Patton, P. M. Frank and R. N. Clark, Fault diagnosis in dynamic systems, theory and application, Control Engineering Series, *Prentice Hall*, London, 1989.
- [21] P. M. Frank, Fault diagnosis in dynamic systems using analytical and knowledge-based redundancy: A survey and some new results, *Automatica*, Vol. 16, No. 3, 1990.
- [22] J. Chen, R. J. Patton and H. Y. Zhang, Designing of unknown input observers and robust fault detection filters, *International Journal of Control*, Vol. 63, No. 1, pp. 85-105, 1996.
- [23] A. Contin, S. d'Orlando, G. Fenu, R. Menis, and S. Milo, Fault detection on a real three-phase induction motor: simulation and experimental results on residual generation, *Proceedings of the 40th IEEE Conference on Decision and Control*, Orlando, Florida, USA, December 2001
- [24] P. P. Harihara, K. Kim, and A. G. Parlos, Signal-based versus model-based fault diagnosis - A trade-off in complexity and performance, *SDEMPED 2003 Symposium on Diagnostics for Electric Mashines, Power Electronics and Drives*, Atlanta, GA, USA, 24-26 August 2003

- [25] S. Abourida, C. Dufour, J. Bélanger, al. et., Real-time PC-based simulator of electric systems and drives. *Opal-RT Technologies Inc.*, 1751 Richardson, 2525, Montreal (Quebec), H3K 1G6, Canada
- [26] C. Dufour, J. Bélanger, al. et., Advances in real-time simulation of fuel cell hybrid electric vehicles. *Proceedings of the 21st Electric Vehicle Symposium(EVS-21)*, April 206 2005, Monte Carlo, Monaco
- [27] C. Dufour, S. Abourida, and J. Bélanger, Hardware-In-the-Loop simulation of power drives with RT-Lab, *Opal-RT Technologies inc.* 1751 Richardson, 2525 Montreal (Quebec), H3K 1G6, Canada
- [28] M. Ouhrouche, R. Beguenane, A.M. Trzynadlowski, J.S. Thongam and M. Dube-Dallaire, A PC-cluster based fully digital real-time simulation Of a fieldoriented speed controller for an induction motor. *International Journal of Modelling and Simulation*
- [29] M. Linjama, T. Virvalo, J. Gustafsson, J. Lintula, V. Aaltonen, M. Kivikoski, Hardware-in-the-Loop Environment for Servo System Controller Design Tuning and Testing, *Elsevier, Microprocessors and Microsystems (24)*, 2000, pp. 13-21.
- [30] J. Chiasson and L. Tolbert, A Library of Simulink Blocks for Real-Time Control of HEV Traction Drives, *Proceedings of the Future Car Congress*, June 3-5, 2002, Arlington, Virginia, USA.
- [31] Opal-RT Technologies Inc., *RT-LAB v7.0 User's Manual*, Opal-RT Technologies Inc., 2002
- [32] P. M. Frank, S. X. Ding, and T. Marcu, Model-based fault diagnosis in technical processes, *Transactions of the Institute of Measurement and Control*, Vol. 22, No. 1, pp. 57-101, 2000.
- [33] X. Lou, Y. Liao, H. A. Toliyat, A. El-Antably and T. A. Lipo, Multiple Couple Circuit Modeling of Induction Machines, *IEEE Transaction on Industrial Application*, Vol 31, pp. 311 -317, Mar/Apr 1995
- [34] Chee-Munong, Dynamic Simulation of Electric Machinery Using Matlab/Simulink. *Prentice Hall PTR*, Upper Saddle River, New Jersey 07458
- [35] K. Trangbak, Linear Parameter Varying Control of Induction Motors, *Ph.D. thesis*, Department of Control Engineering Aalborg University Fredrik Bajers Vej 7 DK-9220 Aalborg, Denmark. ISBN 87-90664-11-6, Doc. no. D-2001-4478, June 2001
- [36] C. T. Kowalski and T. Orłowska-Kowalska, Neural networks application for induction motor faults diagnosis, *Mathematics and Computers in Simulation*, vol. 63, issues 3-5, pp. 438-448, Nov. 2003
- [37] W. W. TAN and H. HUO, An on-line neurofuzzy approach for detecting faults in induction motors, *Department of Electrical and Computer Engineering*, National University of Singapore
- [38] R. J. Patton, P.M. Frank and R.N. Clark, Fault diagnosis in dynamic systems: theory and application. *Prentice Hall International Ltd*, 1989

- [39] P. M. Frank, Fault diagnosis in dynamic systems using analytical and knowledge-based redundancy-A survey and some new results, *Automatica*, Vol. 26, pp. 459-474, 1990.
- [40] J. J. Gertler, Analytical redundancy methods in failure detection and isolation, *Proc. IFAC Symposium SAFEPROCESS'91*, Baden-Baden, 10-13 Sept., pp. 9-21, 1991.
- [41] R. J. Patton, Robust model-based fault diagnosis: the state of the art, *Preprints of IFAC Symposium on SAFEPROCESS'94*, Espoo, Finland, 13-16 June, 1, pp. 1-24, 1994.
- [42] R. Seliger and P.M. Frank, Robust component fault detection and isolation in nonlinear dynamic systems using nonlinear unknown input observers, *Preprints of SAFEPROCESS'91*, Sept. 10-13, Baden-Bade, FRG. 1, pp. 313-318, 1991.
- [43] R. Seliger and P.M. Frank, Fault diagnosis by disturbance decoupled nonlinear observers, *Proc. of 30th IEEE CDC*, Dec.11-13, Briton, U.K., 3, pp. 2248-2253, 1991.
- [44] R. R. Mohler, Bilinear control processes, *Mathematics in Science and Engineering*, 106, Academic Press, 1973.
- [45] K. J. Burnham, D. J.G. James and D.N. Shields, Self-tuning control of bilinear systems, *Optimal control Applications and Methods*, 8, pp. 147-157, 1987.
- [46] I. Derese and E.J. Noldus, Nonlinear control of bilinear systems, *IEE Proc.*, 127, Pt.D, 4, pp. 169-175, 1980.
- [47] S. Hara and K. Furuta, Minimal order state observers for bilinear systems, *Int. J. Control*, 24, 5, pp. 705-718, 1976.
- [48] Y. Funahashi, Stable state estimator for bilinear systems, *Int.J.Control*, 29, 2, pp. 181-188, 1979.
- [49] A. Hac, Design of disturbance decoupled observer for bilinear systems, *Trans.of ASME, J. Dynamic Syst. Measure. Control*, 114, 12, pp. 556-562, 1992.
- [50] D. L. Yu and D.N. Shields, A fault detection method for a nonlinear system and its application on a hydraulic test rig, *Preprints of IFAC Symposium on SAFEPROCESS'94*, Espoo, Finland, 13-16 June, 2, pp. 305-310, 1994.
- [51] D. L. Yu, D.N. Shields and K. Disdell, A Simulation Study on Fault Diagnosis of a High Temperature Furnace Using a Bilinear Observer Method, *Control Eng. Practice*, Vol. 4, No. 12, pp. 1681 - 1691, 1996
- [52] S. H. Wang, E. J. Davision and P. Dorato, Observing the states of systems with unmeasurable disturbance, *IEEE Transactions on Automatic Control*, Vol. 20, pp. 716-717, 1975.
- [53] J. Chen and R. J. patton, Robust Model-Based Fault Diagnosis for Dynamic Systems, *Kluwer Academic Publisher*, Boston, pp. 3107-3112, 1999.

- [54] F. W. Fairman, S. S. Mahil, and L. Luk, Disturbance decoupled observer design via sigular value decomposition, *IEEE Transactions on Automatic Control*, 29, pp. 84-86, 1984.
- [55] Y. Park, and J. L. Stein, Closed-loop, State and inputs observer for systems with unknown inputs, *International Journal of Control*, 48, pp. 1121-1136, 1988
- [56] J. Wünnenberg, Observer-Based Fault Detection in Dynamic Systems, *VDI-Fortschrittsber.*, VDI-Verlag, Reihe 8, Nr. 222. Düsseldorf, Germany, 1990.